



HAL
open science

Temporal and spatial evolution of orogens: a guide for geological mapping

Camille Francois, Manuel Pubellier, Christian Robert, Cédric Bulois, Siti Nur Fathiyah Jamaludin, Roland Oberhänsli, Michel Faure, Marc R. St-Onge

► To cite this version:

Camille Francois, Manuel Pubellier, Christian Robert, Cédric Bulois, Siti Nur Fathiyah Jamaludin, et al.. Temporal and spatial evolution of orogens: a guide for geological mapping. Episodes Journal of International Geoscience, 2022, 45 (3), pp.265-283. 10.18814/epiugs/2021/021025 . hal-03356654

HAL Id: hal-03356654

<https://hal.science/hal-03356654>

Submitted on 11 Jan 2022

HAL is a multi-disciplinary open access archive for the deposit and dissemination of scientific research documents, whether they are published or not. The documents may come from teaching and research institutions in France or abroad, or from public or private research centers.

L'archive ouverte pluridisciplinaire **HAL**, est destinée au dépôt et à la diffusion de documents scientifiques de niveau recherche, publiés ou non, émanant des établissements d'enseignement et de recherche français ou étrangers, des laboratoires publics ou privés.

Temporal and spatial evolution of orogens: a guide for geological mapping

Camille François (1,*), Manuel Pubellier (1,2,*), Christian Robert (2), Cédric Bulois (2,3), Siti Nur Fathiyah Jamaludin (4), Roland Oberhänsli (5), Michel Faure (6), Marc R. St-Onge (7) and the IGCP 667 Team (8)

¹ Commission for the Geological Map of the World – France

² Laboratoire de Géologie - CNRS UMR 8538, École Normale Supérieure - PSL University – France

³ Université Côte d'Azur, IRD, CNRS, Géoazur – France

⁴ Universiti Teknologi Petronas – Malaysia

⁵ Potsdam University – Germany

⁶ Univ. Orléans, CNRS, BRGM, ISTO, UMR 7327, F-45071 Orléans – France

⁷ Geological Survey of Canada, 601 Booth Street, Ottawa, Ontario K1A 0E8 – Canada.

⁸ <https://ccgm.org/en/content/11-team>

* Corresponding authors, email addresses: c.francois.geology@orange.fr (C. François),
manupub.pubellier@gmail.com (M. Pubellier)

Abstract

Orogens develop in convergent settings involving two or more continental and/or oceanic plates. They are traditionally defined as zones of crustal deformation associated with mountain building resulting from either the accretion of an arc, a continent-continent collision or the inversion of a rift basin. However, this somewhat narrow definition does not consider for example the genetic link between an oceanic domain and an intra-continental rift, even though extension associated with a scissor-shape opening can be demonstrated in many ocean-floored basins. Consequently, we propose a new concept of orogenic evolution based on the development of extensional margins subsequently subjected to crustal shortening. Thus orogens that develop as a result of the closure of wide basins, and involve the shortening of supra-subduction basins and arcs, are distinguished from mountain belts developed above subduction zones or that result from continental collision. Inverted intra-continental rifts (devoid of oceanic material) are also considered. Our review of a number of key orogens identifies apparent similarities and differences in geodynamic processes through geological time and emphasizes the lateral spatial and temporal changes that may occur from a subduction to a collisional setting, with such changes being intrinsic to the transition from intra-continental rifts to large basins floored by oceanic crust. We also review the geodynamic processes that operated prior to the onset of plate tectonics. As we go back in time, key tectonic attributes are apparently lost in many cases (but tellingly not all) due to a lack of data, a lack of understanding, or the deeper levels of erosion generally associated with older orogens.

We propose that mapping utilizing tools based on comparative tectonics to understand old terrains and fault zones is a good way to constrain such an evolution and that this can start with a global-scale map of past-to-modern orogens, aimed at re-exploring mountain building concepts spatially and temporarily. This is the primary objective of IGCP 667 project “World Map of Orogens”.

46 **1. Introduction**

47 Orogens form along (or in proximity to) lithospheric plate boundaries in a convergent
48 setting (i.e. subduction, collision) and often involve two or more neighboring continental and/or
49 oceanic plates. On the other hand, intracontinental orogens develop in an intraplate setting. The
50 evolution of an orogen is a complex geodynamic process punctuated by several tectonic events
51 that can be viewed as the “orogenic cycle”, and in which an “orogeny” *sensu stricto* is a
52 fundamental step (**Fig.1**; *Wilson et al., 2019*). Orogenic belts may be defined as a combination
53 of folding, faulting, regional metamorphism and igneous activity within contemporaneously
54 uplifted terranes (*Kearey, 1993*). These orogenic components are found in belts resulting from
55 either continent-continent collision or continental-island arc accretion leading to crustal
56 thickening. These two tectonic settings control the final orogenic architecture through
57 geological processes both at depth and at the surface, including for example: the inversion of a
58 passive margin, the emplacement of tectonic nappes, strike-slip faulting, the accretion of
59 volcanic arcs, granitic magmatism, suture zone deformation and regional metamorphism (*van*
60 *der Pluijm and Marshak, 2004*). Nevertheless, it remains key to differentiate accretionary
61 orogens (*Sengör and Okuurogullari, 1991*), where there is sequential amalgamation of terranes
62 to a continental margin (e.g. the Cenozoic North American Cordillera or the Paleozoic Altaids
63 Belt in Central Asia), from collisional orogens (*Windley, 1999*) where subduction leads to
64 ocean-continent convergence (e.g. Andes of South America) and then continent-continent
65 collision (e.g. Himalaya).

66 The definition of an orogen therefore becomes conceptually important and this obliges us to
67 reconsider the identification of the key diagnostic attributes of an orogeny. It also requires an
68 accurate portrayal of such orogenic attributes on a geological or tectonic map including their
69 location relative to craton boundaries and any older orogen. Such an approach emphasizes the
70 evolutionary steps responsible for continental growth and underline any inherent reactivation

71 process and/or history by documenting the superimposition of orogens through time and space.
72 The resulting parsing of an orogenic belt into key attributes enables the construction of crustal
73 cross-sections, along which overlapping or juxtaposed events can be considered. An important
74 facet of IGCP 667 is thus the investigation of how basins and orogens interact with one another
75 during continental growth, and how that interaction can be considered in terms of geological
76 mapping and map compilations.

77 (Figure 1 is about here)

78 **2. Historical overview**

79 Tectonic displacement from a geological mapping point-of-view was poorly understood
80 until the end of the 19th Century, although vertical movement intrinsic to mountain belt
81 formation was already being considered (*e.g.* theory of mountain systems of de Beaumont
82 (1852); geosyncline theory of Hall and Dana (1873); eustatic variations of Suess (1893)). The
83 first use of the terms “orographic” as applied to a mountain structure in a descriptive sense and
84 “orogenic” in a genetic sense was made by Gressly (1840) and Thurmann (1854) in the Jura
85 Mountains of France. A fundamental step in the establishment of tectonics as an individual
86 science occurred with the geometric description of folds and faults responsible for stratigraphic
87 inversions in the Appalachians of eastern North America by Rogers (1858). Lesley (cited in
88 *Chamberlin and Salisbury, 1906*) further advanced our understanding of mountain belt
89 structures by imagining the horizontal forces required to form large-scale folds, without
90 however defining their specific nature. De Beaumont’s theory of mountain systems somehow
91 evokes the equivalent of an orogeny in the mid-19th Century, but the collage of stratigraphic
92 terranes was not sufficient to explain the formation of mountain belts. Crustal movement as a
93 result of deformation was first theorized by the end of 19th Century by Gilbert (1890) with the
94 formulation of orogenic and epeiorogenic uplift concepts, and in particular the relationship
95 between fold-and-thrust mountain belts and lateral-compressional tectonics. However, Gilbert

96 (1890) attached no specific time connotation to an orogeny. The concept of orogeny as “the
97 process of mountain-building” was first developed by Upham (1894) who defined orogeny as
98 “denoting the process of formation of mountains ranges by folds, faults, upthrusts and
99 overthrusts, affecting comparatively narrow belts and lifting them in great ridges”. Later, Haug
100 (1907) distinguished four major orogenies: Huronian (end of Precambrian), Caledonian (Early
101 Paleozoic), Hercynian (Late Paleozoic) and Alpine (Cretaceous). Stille (1920) reconsidered
102 orogenesis as an episodic change in the rock deformation fabric, thus equating the term to both
103 an event and a tectonic process. The definition of orogeny proposed by Stille (1940) involved
104 the pervasive deformation of pre-existing rock fabrics, limited in space and time and hence
105 implying a spatiotemporal event, was widely accepted.

106 Major orogens are commonly generated by continental collisions, but these can be
107 superimposed through time and space thus potentially masking key information on the
108 fundamental nature of the shortening processes involved. The understanding and classification
109 of such processes therefore becomes crucial and includes documenting the reactivation of older
110 tectonic features during mountain building, as well as in any subsequent ocean opening. It
111 therefore becomes important to revisit the concept of orogeny and to also identify potential
112 continental growth through mantle extraction processes through time and space.

113 The present overview of the world’s orogens is part of the ongoing IGCP 667 Project “World
114 Map of Orogens”, in which the main driver is to design a map at scale 1:35 000 000
115 documenting the distribution of ancient to modern orogens throughout Earth history. The
116 compilation of a “World Map of Orogens” necessarily requires a careful consideration of both
117 the various types of global-scale compressional tectonic regimes and the best means of
118 portraying the associated tectonic elements or attributes on such a map. Consideration of pre-
119 plate tectonic, Early Earth crustal deformation processes and features also becomes necessary.
120 As we go back in time, we propose a slight simplification of the main tectonic attributes

121 captured due to an increasing paucity of data. We conclude by presenting a number of orogens,
122 from the Paleoproterozoic to the present, with a legend that includes the key elements of a
123 “typical” orogen.

124 **3. A four-fold geodynamic classification of orogens**

125 Recent evolutionary models of continental margins and basins (*d’Acremont et al., 2006;*
126 *Fournier et al., 2010; Franke et al., 2014; Pubellier et al., 2016; Bulois et al., 2018*), as well as
127 comparisons between modern and ancient orogenic systems (e.g. *Weller and St-Onge, 2017;*
128 *Brown and Johnson, 2018; Palin et al., 2020*), emphasize the notions of margin evolution, basin
129 development, rift propagation and basement reactivation. In the documentation of most
130 orogenic systems, a space-time continuum of deformation affecting the various geological
131 elements of a mountain belt is reported. This continuity of tectonic events can be directly linked
132 to the Wilson Cycle (**Fig.1**). Given the current understanding that geological processes are
133 intimately linked to orogenic evolution, it seems timely to propose a different geodynamic
134 classification of orogens in order to emphasize the overall tectonic processes occurring during
135 lithospheric shortening.

136 Four main types of convergent orogenic systems can be identified within the present-day
137 geodynamical settings encountered on Earth (**Fig.2**): (i) ocean-continent convergence
138 accommodated by subduction, (ii) accretion/collision of crustal elements derived from
139 subduction (island arc and/or back-arc basin), or occurring as a microcontinent, ribbon
140 continent, oceanic plateau or ridge, (iii) continental collision, often following subduction ±
141 accretion and (iv) shortening of an intracontinental sedimentary basin and continental crustal
142 materials. Each of these types in turn may only represent one step in the development of an
143 orogen in time and space, thus a transition between each stage can/should be considered. Indeed
144 most of these orogens will result in construction of topography, particularly the continental
145 collision, which is followed by orogenic collapse along large low angle normal faults, which

146 are generally located at the frontier between zones of strongly varying rheologies. This post
147 orogenic stage aspect is not developed in the synthesis.

148 Type I (**Fig.2a**) involves ocean-continent convergence and leads to the formation of a
149 mountain belt on the overriding upper plate, as a result of igneous material sourced from the
150 underlying subduction zone. Compression may happen during oceanic subduction when there
151 is a change in subduction attributes such as the dip or the relative velocity of the subducting
152 slab, the obliquity of the convergence, or the amount of sedimentary material deposited in the
153 trench, underplated or subducted with the downgoing plate. This results in a non-collisional
154 system typical of Andean-type cordilleras (South America, Eastern Australia, and Antarctica).
155 The Type I orogen is often considered as a precursor to continental collision (cf Type III), so
156 that the resulting mountain range built on the upper plate can be referred to as the “early-
157 orogenic zone”.

158 Type II (**Fig.2b**) involves micro- or ribbon-continents and slivers of the continental
159 margin rifted during the opening of back-arc basins. The slivers may also include oceanic
160 plateaus (e.g. Olong-Java in the Solomon Islands), exotic island arc terranes (e.g. North
161 American Cordillera) or continental accreted terranes (e.g. Cascadia). The convergent process
162 is often known as terrane docking or accretion and it results in a tectonic collage of pericratonic
163 and suspect terranes (*Coney et al., 1980; Howell, 1989*). The accretion of pericratonic, suspect,
164 or exotic terranes represents a milestone in the history of an oceanic basin. The orogen forms
165 when a crustal domain is rifted away from a continental margin and eventually reaches an active
166 continental margin. As subduction of the now-accreted crustal domain is not possible,
167 subduction jumps to the opposite side of the docked terrane (e.g. Anatolia, Iran; *Barrier and*
168 *Vrielynck, 2008*, or SE Asia; *Pubellier and Meresse, 2013*). Where observations are more
169 complete (e.g. Cenozoic convergent settings), the docked crustal domains are often back-arc

170 basins floored by continental basement, or island arcs. This stage may therefore be considered
171 as a prelude to the eventual formation of a continental collisional belt (Type III).

172 Type III (**Fig.2c**) is characterized by the collision of two or more continental
173 landmasses. Continental collision, sometimes referred to as “terminal collision” in the literature
174 (e.g. *Najman et al., 2017; Abu Sharib et al., 2019*), is characterized by a pre-collisional history
175 that can involve a lengthy period of subduction and terrane accretion (cf Types I and II).
176 Because of the crustal thickness of the subducting lithosphere and its positive buoyancy, most
177 of the incoming material cannot be subducted, or remain subducted, leading to crustal
178 shortening, accommodated by low-angle syn-metamorphic ductile shearing and orogeny.
179 Therefore, a continent-continent collision follows the complete closure of an oceanic basin (e.g.
180 Himalaya, European Alps) and the closure of the arc and/or back-arc system in the upper plate.

181 Type IV (**Fig.2d**) is an intra-continental orogen formed during the inversion of a rift
182 system that originated from pre-orogenic rifting that never led to the formation of oceanic crust.
183 The Atlas Mountains in NW Africa are a classic example of this type of orogen, in which only
184 the upper structural levels and the metamorphic rocks they contain are exposed (e.g. *Mattauer*
185 *et al., 1977; Beauchamp et al., 1999; Frizon de Lamotte et al., 2000; Missenard et al., 2006*).
186 Another example from the South China Block comprises a Silurian intracontinental orogen, in
187 which deep seated metamorphic zones are exposed. The Early Paleozoic Orogen (EPO) of
188 South China, has long been recognized due to a Devonian unconformity (*Grabau, 1924*). This
189 pre-Devonian belt resulted from the closure of a Neoproterozoic to Ordovician rift within
190 continental crust and without involving oceanic crust (e.g. *Yao et al., 2014*). The rift closure
191 was accommodated by a north-directed continental subduction as shown by south-verging folds
192 and thrusts, and ductile kinematics in the southern part of the belt (*Faure et al., 2008; Charvet*
193 *et al. 2010; Li et al., 2010; Wang et al., 2013; Xin et al. 2020 and enclosed references*). The
194 inner zone of this orogen consists of mid temperature and mid pressure biotite-garnet-staurolite-

195 kyanite metapelites and garnet amphibolites that document P-T conditions at 1.0- 1.2 GPa and
196 500-600°C (*Zhao and Cawood 1999*). The driving force for the intracontinental orogen is
197 interpreted as being the far-field effect of the Ordovician collisional orogeny recognized in
198 central Vietnam, responsible for the welding of the Viet-Cambodia block and the Viet-Lao (or
199 North Vietnam-South China) blocks (*Faure et al., 2018*).

200 Intracontinental orogens may also result from highly oblique continental collisions (e.g.
201 Southern Alps of New Zealand; *Beaumont et al., 1996*). Transpressional components can also
202 play important roles in the formation of intracontinental orogens. In spite of a unique initial pre-
203 orogenic setting, the intracontinental orogens exhibit structural, metamorphic, plutonic and
204 sedimentary features similar to those of type III orogens (cf. Table 1).

205 As a broad generalization, a Type I orogen can often represent an early stage of a Type II or
206 Type III orogen. In this overview, we have defined an “early orogenic zone” (**Table 1**), which
207 can be compared and contrasted to the three other (generally subsequent) orogenic stages and
208 zones: peri-orogenic/orogenic zones (types II and III) and para-orogenic zones (Type IV).

209 The “orogenic zones” in types II and III are associated with the presence of ophiolites, (U)HP
210 and (U)HT metamorphic rocks and plutonism (granites). The “peri-orogenic zones” correspond
211 to areas of more moderate deformation, lower grade metamorphism, moderate topography, the
212 presence of molassic foreland basins as well as fold-and-thrust belts developed above shallow
213 detachment levels. The “para-orogenic zone” (**Table I**), is associated with Type IV orogens and
214 is characterized by moderate deformation along inverted rifted features, occasionally low-grade
215 metamorphism and the exhumation of mantle material without the presence of oceanic crust
216 as a result of the shortening of former propagator tips.

217 (Figure 2 is about here)

218 (Table 1 is about here)

219 **4. The geometry of basins and orogenic implications**

220 During crustal shortening, a previously extended sedimentary basin is often subjected
221 to compression during the process of tectonic inversion. The precise end of the rifting (breakup)
222 is contemporaneous with the first sedimentary units deposited on oceanic crust and can
223 sometimes be confirmed with the presence of clear oceanic magnetic anomalies. The opening
224 is rarely orthogonal, implying an along-strike migration of breakup with time (**Fig.3**). The
225 newly formed oceanic crust is therefore wider at one end and narrower on the opposite end of
226 the newly formed basin. It might even be connected to a continental rift inland, which is devoid
227 of oceanic crust. The resulting V-shape geometry yields strong implications on the style of any
228 subsequent shortening and timing of eventual basin closure.

229 4.1. Non-orthogonal opening of basins, and propagation of rift systems

230 Rift basin opening is rarely orthogonal. Most of the well-documented marginal basins
231 have a scissor-shape geometry resulting from the propagation of a rift toward locked zones
232 (*Courtillet, 1982*). Notable examples include the Woodlark Basin (*Weissel and Watts, 1979*;
233 *Taylor et al., 1999*), the Gulf of Aden (*Courtillet, 1982*; *d'Acremont et al., 2006*; *Fournier et*
234 *al., 2010*) and the South China Sea (**Fig.3**; *Briais et al., 1993*, *Franke et al., 2014*; *Pubellier et*
235 *al., 2016*). In continental rift systems, such as the North Atlantic, a similar along-axis
236 propagation of the deformation is also documented based on paleogeographic reconstructions
237 (e.g. *Ziegler, 1990*) but the absence of clear oceanic crust in some cases (e.g. Gakkel ridge)
238 remains problematic to fully understanding how deformation propagates spatially and
239 temporarily. In general, the propagation of rifts is due to either a lateral variation in the timing
240 of the initial breakup due to local weaknesses of the continental crust, or to the proximity of the
241 Euler rotation pole with the tip of V-shape rifted basin. The breakup point migrates with
242 continued extension as long as the basin is opening (e.g. *Martin 1984*; *Taylor et al., 1999*;
243 *Bellahsen et al. 2003*; *ArRajehi et al. 2010*; *Péron-Pinvidic and Manatschal 2010*; *Fletcher et*

244 *al.*, 2013), so that the breakup unconformity is diachronous along-strike, with break-up ages
245 decreasing in the direction of propagation (*Ding and Li, 2016, Franke et al., 2014; Gaina et*
246 *al., 1999; Bulois et al., 2017*). The integration of field and seismic studies documents that rift
247 propagation slows down or stops when the rift tip abuts transversal structures of orogenic origin
248 (e.g. *Bulois et al., 2018*). Numerical models have shown that tectonic loading in the propagation
249 direction is crucial for slowing down or halting continental rifting and allowing the
250 development of a wide triangular zone of stretching and thinning of the continental crust (*Le*
251 *Pourhiet et al., 2018*).

252 One of the best-documented rift propagator is the South China Sea Basin (*Taylor and Hayes,*
253 *1983*), where all these characteristics are documented. The rift migration (*Franke et al, 2014*)
254 produced a large ocean-floored basin in the NE (Eastern Sub-basin) and a narrow ocean floor
255 in the central part (SW sub-basin) with the tip corresponding to a continental rift south of
256 Vietnam - the Nam Con Son Basin (**Fig. 3a**; *Li et al., 2014, Sibuet et al., 2016*). The subdivisions
257 of the basin reflect interaction with the surrounding continental and oceanic crust, for example
258 in the form of depocenter locations. The opening of the South China Sea is related to
259 neighbouring basins closure (*Pubellier et al. 2013*), implying a constant relocation of tectonic
260 stresses within this portion of the continental crust. As such, it is important to consider that a
261 scissor-shape opening is conditioned by the dynamics of the neighbouring subduction. In larger
262 oceanic basins bounded by well-defined continental margins (e.g. Tasman Sea, Atlantic Ocean;
263 e.g. *Guiraud and Maurin, 1992; Seton et al., 2012a; b*), similar opening mechanisms might be
264 considered, recognizing that these may be masked by subsequent changes in basin boundary
265 conditions.

266 (Figure 3 is about here)

267 4.2. Implications on the geodynamic classification of orogens

268 In oceanic rift systems, the oceanic crust is predominantly associated with exhumed
269 mantle outboard of the continent-ocean transition (COT), and the divergent system transitions
270 laterally to a younger continental extensional domain toward the propagator tip (Fig. 3a, e.g.
271 *Benes et al., 1994; Taylor et al., 1995; 1999; 2009; Goodliffe et al., 1999; Martinez et al.,*
272 *2001; Clift et al., 2002; Minshul, 2009; Franke et al., 2014; Li et al., 2014*). This type of
273 geological setting promotes a scissor-like opening of the extensional basin, with an oceanic
274 basin forming away from the propagator tip and a continental rift or aulacogen forming at the
275 propagator tip. This transition occurs in several steps controlled by transfer faults near the COT
276 and larger transform faults in the oceanic domain. This is particularly well documented in recent
277 rift propagators such as the South China Sea, the Woodlark Basin, the Gulf of Aden and the
278 Gulf of Mexico. It is also envisaged for the Proto-Tethys Ocean in the Early Paleozoic (*Scotese,*
279 *2016*), as well as for the Paleo-Tethys in the Late Paleozoic (*Stampfli and Borel, 2001*). In the
280 case of the Neo-Tethys Ocean, it appears that the continental blocks that rifted away from the
281 main continent were larger in the East where the ocean was wider (*Borel and Stampfli, 2002,*
282 *Scotese, 1991, Pourteau et al., 2009*), resulting in wider Phanerozoic Tethysides (*Sengör et al.,*
283 *1996*).

284 The above extensional mechanisms imply along-strike time-variation of opening, which is
285 reflected in the distance between the opposite conjugated margins. If this V-Shape geometry is
286 spectacular in the South China Sea or the Woodlark Basin, it is also the case for the large but
287 simple example of the Atlantic Ocean, which opened in a northward direction from the Early
288 Cretaceous to the Eocene where it ends as a rift at the tip along the Gakkel Ridge.

289 In any theoretical subsequent plate convergence, the required time for the basin margins to close
290 will produce a reverse migration of the locus of closure along strike, with early collision in the
291 rift system to later subduction-accretion followed by continental collision toward the open end
292 of the V (**Fig. 3b**). In other words the timing of collision should be diachronous along strike,

293 with resulting differences in the time of deformation of the accretionary wedges, as well as the
294 formation of the post-orogenic molassic basins. Such a scenario also implies that the material
295 engulfed in the collision zone evolves laterally from an accretionary wedge to a continental
296 wedge as is documented from the Eastern Sunda wedge to the Burma-Bangladesh fold-and-
297 thrust belt, or from the Muertos wedge to the Haïti fold-and-thrust Belt in Hispaniola. Intra-
298 oceanic deformation prior to collision and ophiolite obduction would take place in that part of
299 the oceanic realm that was formerly wide, while no oceanic or ultramafic material would be
300 found in the intra-continental rift region. This type of along-strike variation is observed in the
301 western Pyrenees where the oceanic-floored V-shaped Bay of Biscay is expressed inland as
302 shortened packages of serpentinized mantle within the orogenic belt (*Jammes et al. 2004*;
303 *Lagabrielle and Bodinier, 2008*; *Tugend et al., 2014*).

304 **5. Temporal evolution of orogens**

305 5.1. Early Earth geodynamic processes (before 2.5 Ga)

306 Today, the global tectonic regime is dominated by plate tectonics or mobile-lid tectonics
307 including deep and cold subduction and/or collision. However, the early Earth (> 2.5 Ga) was
308 subject to a very different, higher mantle heat flux and a thermal regime characterized by the
309 formation of unique lithomagmatic assemblages including the emplacement of tonalite-
310 trondjemite-granodiorite (TTG) suites in the early continental lithosphere and the formation
311 of granite-greenstone terrains (*e.g. Arndt and Nisbet, 1982*; *Abbott and Hoffman, 1984*; *Taylor*
312 *and McLennan, 1985*; *Abbott et al., 1994*; *Jaupart et al., 2007*; *Coltice et al., 2009*; *Gapais et*
313 *al., 2009*; *Bédard and Harris, 2013*; *Bédard, 2018*; *Tang et al., 2019*; *Chen et al., 2019*; *Roman*
314 *and Arndt, 2019*; *Hernández-Montenegro et al., 2021*). Accordingly, the early Earth was
315 dominated by different geodynamical processes (**Fig.4**), including flat or low angle subduction
316 (mobile-lid tectonics; *Smithies et al., 2003*) and sagduction (stagnant-lid tectonics; *McGregor,*
317 *1951*). Sagduction is thought to have been driven by partial convective overturn due to the

318 density contrast between dense (ultra) mafic cover (greenstone belts) and the more felsic crustal
319 basement (TTG), coupled with partial melting in the lower crust (*Collins et al., 1998; Van*
320 *Kranendonk et al., 2004; Thébaud and Rey, 2013; François et al., 2014; Bédard, 2018; Roman*
321 *and Arndt, 2019*). This resulted in the typical Archean dome-and-keel structures with TTG
322 terrains forming ovoid domes surrounded by narrow and strongly pinched greenstone belts.
323 Such a configuration is not suggestive of large tangential movements of plates, and the complete
324 absence of ultra-high pressure (UHP) metamorphic assemblages also suggest a completely
325 different geodynamic regime (*Brown and Johnson, 2018*). In addition, the very local evidence
326 of Archean (flat) subduction is rare and controversial (*Volodichev et al., 2004; Moyen et al.,*
327 *2006 Perchuk and Morgunova, 2014*). It would seem that the thermal (i.e. a higher mantle heat
328 flux) and the rheological conditions prevalent during the Archean Eon probably made modern
329 steep subduction (burial of a lithospheric panel at great depth) impossible.

330 The Archean metamorphic rock record and implied pressure-temperature (PT) conditions
331 (apparent geothermal gradient) can be used to discriminate geodynamic processes in the early
332 Earth, and more particularly to infer whether or not deep and cold subduction similar to that of
333 modern plate tectonics was operational (*Brown, 2008; Brown and Johnson, 2018*). The oldest
334 evidences of high pressure (HP) rocks (> 15 kbar) are bracketed between 2.2 and 1.8 Ga (e.g.
335 *Möller et al., 1995; Baldwin et al., 2004; Collins et al., 2004; Volodichev et al., 2004; Boniface*
336 *et al., 2012; Weller and St-Onge, 2017; François et al., 2018; Loose and Schenk, 2018; Xu et*
337 *al., 2018; De Olivera Chavez, 2020*). Consequently, these authors suggest a beginning for
338 modern-style plate tectonics and therefore orogens (as per the types presented above) at or
339 following 2.5 Ga (*St-Onge et al., 2006; Shirey and Richardson, 2011; François et al., 2018;*
340 *Brown and Johnson, 2020*). It is for this reason that we decided to document orogens and their
341 attributes post 2.5 Ga and to represent old geodynamic features (i.e. Archean dome-and-keel
342 structures) in the craton map (**Fig.4**).

343 (Figure 4 is about here)

344 5.2. “Modern” orogens (after 2.5 Ga)

345 The convergent margin geodynamic processes that developed after the end of the
346 Archean continued to undergo a progressive change as a result of the continued secular cooling
347 of the Earth. Younger mountain belts show better-preserved components allowing a better
348 definition of successive tectonic events with time. As a result, there may be a bias in the
349 apparent extent of orogens with age. We choose to illustrate this aspect with examples from the
350 Trans-Hudson, the Caledonian, the Variscan-Uralian and the Alpine systems, which show
351 somewhat finer resolution with time. In all these examples, we restrict the definition of an
352 “orogen” to spatial areas affected by tectonics events within and on the borders of former oceans
353 that played a key role in the development of the crustal features related to ocean closure.

354 5.2.1. *Trans-Hudson orogeny and closure of the Manikewan Ocean*

355 The middle to late Paleoproterozoic, and specifically the aptly named Orisirian Period
356 (2015-1800 Ma), is believed to have witnessed the assembly of Earth’s first genuine
357 supercontinent variably referred to as either Nuna, Columbia, or Hudsonland (*Piper, 1976;*
358 *Hoffman, 1988, 1997; Park, 1995; Meert, 2002, 2012, 2014; Pesonen et al., 2003*). The primary
359 evidence for Nuna is based on paleomagnetic data and on comparative geology, and observed
360 through alignment and broad synchronicity of geological features including mafic dyke
361 swarms, rift and continental-margin supracrustal sequences, suture zones, oceanic and
362 continental magmatic arcs, obducted ophiolites, thrust and fold belts, localities of high- and
363 ultrahigh-pressure metamorphism, and in particular 2.00–1.74 Ga orogenic belts on a majority
364 of the continents (**Fig. 5**; *Zhao et al., 2002, 2004, 2011; Evans and Mitchell, 2011; Evans et*
365 *al., 2016; Meert and Santosh, 2017; de Oliveira Chaves et al., 2020; Wan et al., 2020*).

366 The largest of the Nuna-affiliated orogenic belts is the ca. 1.92–1.74 Ga Trans-Hudson orogen
367 (*Hoffman, 1988; Lewry and Stauffer, 1990*), which comprises superbly exposed erosional
368 remnants of a collisional mountain belt that extended ~3,000 km across North America into
369 northeastern Arctic Canada (**Fig. 5**). In Greenland, the continuation of the Trans-Hudson
370 orogen is the well-studied, but largely ice-covered, Nagssugtoqidian orogen (**Fig. 5; van Gool**
371 *et al. 2002; Connelly et al. 2006; Nutman et al., 2008a; St-Onge et al., 2009; Garde and Hollis,*
372 *2010; Kolb, 2014; and references therein*). Further to the east, the Trans-Hudson orogen is
373 manifest as the Lapland-Kola orogen in Baltica (**Fig. 5; Daly et al., 2006; Korja et al., 2006;**
374 *Lahtinen et al., 2008; Petrov et al., 2018; Lahtinen and Huhma, 2019*). In Canada, numerous
375 studies of the Trans-Hudson orogen have shown that it formed during progressive closure of
376 the Manikewan Ocean and accretion of intervening suspect terranes, culminating with the
377 collision of the lower-plate Archean Superior craton with an upper-plate collage of Archean
378 and Paleoproterozoic crustal blocks (collectively known as the Churchill plate) at ca. 1.82 Ga
379 (*St-Onge et al., 2006, 2007, 2009, 2020; Corrigan et al., 2009; Corrigan, 2012; Weller and St-*
380 *Onge, 2017; Dumond, 2020; Weller et al., 2020; and references therein*). Several parallels have
381 been drawn between the Trans-Hudson orogen and the archetypical Himalayan orogen of
382 central Asia as both orogens are of a similar scale and exhibit similar patterns of magmatism
383 and metamorphism with respect to the timing of collision (*St-Onge et al., 2006; Eaton and*
384 *Darbyshire, 2010; Thompson et al., 2010; Bastow et al., 2011; Corrigan, 2012; Weller and St-*
385 *Onge, 2017*).

386 Signature tectonic features that characterize Trans-Hudson orogen include mounting evidence
387 for continental subduction during diachronous plate convergence as documented by high- to
388 ultrahigh-pressure/low-temperature mineral assemblage localities, and closure of intervening
389 oceanic domains as witnessed by obducted ophiolitic suites. Within the Trans-Hudson orogen
390 of Laurentia and Baltica (**Fig. 5**) well-researched Paleoproterozoic eclogite localities include:

391 the 1.83 Ga Kovik eclogite (*Weller and St-Onge, 2017*), the 1.87 Ga Kuummiut eclogite
392 (*Nutman et al., 2008b; Müller et al., 2018*) of SE Greenland, and the 1.9 Ga Belomorian eclogite
393 (*Yu et al., 2017*) of western Russia. Taken as a set, the Trans-Hudsonian eclogites record a
394 clear east-to-west diachronous trend in the age of continental subduction and orogenesis, and
395 by inference, Manikewan Ocean closure.
396 (Figure 5 is about here)

397 5.2.2. Caledonian orogeny and closure of the Iapetus Ocean

398 On the northern British Isles, during the Early-Middle Ordovician (c. 470-460 Ma), a
399 volcanic island arc (the Midland Valley arc terrane) that had formed along the margins of the
400 Iapetus Ocean, collided with Laurentia (**Fig.6**). This marked the onset of the Grampian phase
401 of the Caledonian orogeny (*Strachan & Woodcock, 2021*). Sedimentary and igneous rocks
402 trapped between the colliding landmasses were intensely folded and faulted and subject to
403 varying degrees of regional metamorphism (*Smooth, 2012*).

404 The subsequent (or continuing) Scandian phase of the Caledonian orogeny, which occurred
405 from the Ordovician to the Middle Silurian (450-430 Ma), resulted in full closure of the Iapetus
406 Ocean and amalgamation of Laurentia, Baltica and Avalonia to form Laurussia (**Fig.6**). Early
407 phases of deformation and/or metamorphism are recognized in the Scandinavian Caledonides
408 and resulted from eastern Avalonia moving independently towards Baltica during the
409 Ordovician. This motion was accommodated by the subduction of the southeastern Iapetus
410 Ocean (so called Tornquist Sea) beneath Avalonia. The continental collision between Avalonia
411 and Baltica began in the Late Ordovician, about 450 Myr ago (**Fig.6**). As a result, the Tornquist
412 Sea was consumed and the resulting suture became the Tornquist Line. This was followed by
413 another phase of deformation and low-grade metamorphism during the Early Devonian (c. 405-
414 395 Ma), known as the early Acadian phase in the present-day NW North American and NE
415 European Atlantic margins. Clearly then, the Iapetus Ocean first closed in the north (*Robert et*

416 *al.*, 2020) with continued closure migrating south and resulting in a diachronous collisional
417 orogeny.

418 (Figure 6 is about here)

419 5.2.3. Variscan-Uralian orogenies and closure of the Rheic and Uralian oceans

420 The closure of the Paleozoic oceans that extended from Mexico to Central Asia gave
421 rise to the Pangea supercontinent. To a certain extent, the resulting orogenies may also include
422 the Acadian and Alleghanian belts in North America, but the main orogenic segment is usually
423 referred to as the Variscan Orogen, which is well documented in Western Europe, from Iberia
424 and Cornwall to Bohemia. The Variscan belt is also represented in basement domains to the
425 Alpine orogen but its distribution is still poorly understood.

426 The late Acadian Orogeny (375-325 Ma) resulted from the collision of an island arc with
427 Laurussia. It was followed by the Alleghenian Orogeny (325-260 Ma) driven by the collision
428 between Laurussia and Gondwana. Together, both orogens formed the Ouachita and part of the
429 Appalachian Mountains in North America, as well as the Moroccan Meseta and the Anti-Atlas
430 in north-western Africa, a once continuous orogenic belt prior to the opening of the Atlantic
431 Ocean starting in Triassic times (*Michard et al.*, 2020).

432 The Variscan orogen of Southern Britain and Western Europe is related to the closure of several
433 oceanic basins of unknown width between Laurussia in the north and Gondwana in the south
434 (in the present coordinates). Some intervening microcontinents are also recognized between the
435 two large convergent continents (*e. g. Matte, 1986, 2001; Pin, 1990; Faure et al. 2005, 2008;*
436 *Martinez-Catalan et al. 2009; Ballèvre et al., 2009, Lardeaux et al., 2014*). In spite of several
437 controversies on the spatial extent and age of the oceanic domains related to the Variscan
438 orogeny, the Saxothuringian and Armorican microcontinents are interpreted as pericratonic to
439 the Gondwanian margin, rifted in the Early Ordovician (ca 480-460 Ma), and containing
440 evidence of the Neoproterozoic Cadomian orogeny. From the inner to outer parts of Gondwana,

441 three oceanic domains are recognized. i) The Medio-European (also called Galicia-Massif
442 Central) Ocean was probably a small basin similar to the present Red Sea, on the basis of similar
443 benthic faunas on both sides of the ocean. ii) The Tepla - Le Conquet Ocean separated the
444 Armorican and Saxothuringian blocks. iii) Lastly, the Rheic Ocean was the main oceanic basin
445 separating Laurussia and Saxothuringia, and the widest due to the presence of different faunal
446 assemblages observed on the Laurussia and Gondwana sides. The timing of closure for these
447 oceanic basins remains disputed. Some authors argue for a poly-orogenic evolution whereas
448 others argue for a monophased collision. In the monocyclic model, all three oceans closed in
449 the Late Devonian-Early Carboniferous, whereas, in the polycyclic model, the Medio-European
450 Ocean was closed by an early oceanic subduction below Armorica. The Gondwana-Armorica
451 Early Devonian collision gave rise to the eo-Variscan belt characterized by HP-UHP
452 metamorphic rocks (eclogites and granulites), SW-directed synmetamorphic nappes, and
453 crustal melting. In the Variscan orogeny, the main collisional event took place when both the
454 Rheic and Tepla-Le Conquet oceans closed after south-directed subductions in Late Devonian-
455 Early Carboniferous, at ca 360 Ma. Late collisional tectono-metamorphic events developed
456 from Viséan to Serpukhovian (ca 335-320 Ma). This deformation produced a doubly-vergent
457 orogen, i.e. north- and south-directed folds and thrusts on the north and south sides of the
458 orogenic belt, respectively. Due to the Permian Ibero-Armorican orocline, the northern foreland
459 developed from the Rheinische Schiefer Gebirge of eastern Germany, through the Ardennes,
460 SW England, and southern Portuguese zone of Iberia with various displacement directions. The
461 continuity of the southern foreland basin, well exposed in southern France (Massif Central,
462 Pyrenees), SE Spain, and SW Sardinia, was disrupted by the opening of the Provence-Algeria
463 basin in the Neogene. Of interest is the fact that the Paleotethys Ocean is not recognized to the
464 west of Turkey, and therefore did not play a significant role in the formation of the Variscan
465 orogen.

466 The Uralian orogen was the consequence of the Permian closure of the Uralian Ocean between
467 Laurussia in the west and Siberia in the east. The former comprises the subducting plate,
468 whereas the latter was the upper plate, upon which a magmatic arc was built (*Puchkov, 2009*).
469 The southwestern margin of Baltica defined by the Trans European Suture Zone represents an
470 Early Paleozoic suture (sometimes referred to as the “Polish Caledonides”), possibly reworked
471 by strike-slip faulting in the Late Paleozoic. To the southeast of Baltica, the Uralian orogen
472 formed when Laurussia and Kazakhstania collided with Siberia in the late Carboniferous to
473 early Permian.

474 The eastern extension of the Variscan orogen in Central Asia remains poorly documented and
475 is beyond the scope of the present contribution. The Central Asia Orogenic Belt (CAOB) is the
476 consequence of multiple microcontinent collisions between the Siberia, Tarim, and North China
477 Block (**Fig.7**; *Sengor et al., 1996*; *Sengor and Natal'in, 1993*; *Xiao et al. 2008*; *Choulet et al.,*
478 *2012*). However, another Paleozoic ocean developed at the location of the Kunlun orogen
479 between the Tarim and Qaidam blocks and was connected to South China and Indochina seas.
480 (Figure 7 is about here)

481 5.2.4. *Alpine orogeny and closure of the Neo-Tethys and Alpine Tethys oceans*

482 The complex history of the Alpine cycle begins with the opening of the Triassic
483 (Carnian, 220 Ma) Meliata-Maliac Ocean, followed by the opening of the Vardar Ocean in the
484 Jurassic (Toarcian-Aalenian, 180 Ma), later referred to as Neo-Tethys (east) and Alpine Tethys
485 oceans (*Stampfli, 2000*; *Bousquet et al., 2008*). In the Western Alps, the Liguro-Piemonte ocean
486 opened in Middle Jurassic (Callovian-Oxfordian). The complexity of the Alpine orogeny
487 comes from the fact that ~~the~~ its history is intrinsically related to the diachronous closure of two
488 oceanic systems, the Neo-Tethys Ocean (eastern domain) and the Alpine Tethys Ocean
489 (western domain ; *Stampfli, 2000* ; *Bousquet et al., 2008*) when Africa ~~and India~~ collided with
490 Eurasia. Convergent plate movement began in the early Cretaceous, but the major phases of

491 mountain building occurred from the Paleocene to the Eocene, and continues today (**Fig.8**; refs).

492 The Alpine Orogen *sensu lato* includes all the Tethyan system from the Moroccan Atlas to the

493 Himalaya.

494 The Alpine Tethys comprises the Piemont-Liguria Ocean and the Valais Ocean. These are

495 extensions of the Atlantic Ocean continuing eastward into the area of the Circum-Mediterranean

496 orogens during rifting and drifting. The Piemont-Liguria Ocean becomes an extension of the

497 Central Atlantic by Middle Jurassic time. In turn, the Valais Ocean (northeast of the

498 Briançonnais microcontinent) forms a Northern Atlantic extension by Middle Cretaceous time.

499 The opening of the Piemont-Liguria Ocean led to separation of the Adria plate from the

500 European continent in Callovian-Oxfordian time (165-156 Ma) and its closure forms the suture

501 zone between the Austro-alpine nappes (derived from Adria) and the Briançonnais

502 microcontinent. Contemporaneously, the Triassic Meliata-Maliac Ocean subducted

503 southeastward beneath the Jurassic upper plate portions of the Neo-Tethys Ocean (ophiolitic

504 units from Vardar that later formed the Dinarides). By Cretaceous times, the closure of Meliata-

505 Vardar produced the Eastern Alps orogeny (*Schmid et al., 2008; Bousquet et al., 2008; Handy*

506 *et al., 2014*).

507 In Santonian time the two branches of the Alpine Tethys (Valais and Piemont-Liguria) were

508 connected *via* the Carpathian embayment with the younger part of Neo-Tethys (Cretaceous in

509 age), leading to a back-arc ocean that formed the future Sava Zone of Dinarides, which is

510 considered a remnant of the Vardar Ocean. By Tertiary time, closure of the Alpine Tethys

511 produced the Western and Central Alps orogeny (*Bousquet, 2008, Handy et al., 2010, 2014;*

512 *Schmid et al., 2019*). Further east the Caucasian-Arabian belt is part of the late Cenozoic

513 Alpine-Himalayan belt. The Trans-European Suture Zone-Kopetdag-Caucasus megafault

514 separates the alpine orogen and the Eurasian plate. The Caucasian-Arabian segment consists of

515 the Greater Caucasus to the north and the Caucasian-Arabian Syntaxis to the south. Greater

516 Caucasus represents the southern margin of the Eurasian plate uplifted over the Main Caucasian
517 Fault (part of the Trans-European Suture Zone-Kopetdag-Caucasus megafault). The Caucasian-
518 Arabian Syntaxis is a zone of indentation of the Arabian plate into the southern East European
519 craton and the Alpine structure of the Caucasus is generated by the interaction of the Arabian
520 indenter and the East European craton. By the late Cenozoic this interaction lead to a 200 to
521 400 km shortening of the Caucasian-Arabian Syntaxis (*Sharkov et al., 2015*).
522 Therefore, in a tectonic sense the Alpine orogen (*lato sensu*) is the result of two orogenies
523 associated with closure of two oceanic systems: Meliata (Neo-Tethys) by the end of Cretaceous
524 time and Alpine Tethys (Atlantic) during Tertiary time.
525 (Figure 8 is about here)

526 **6. Key orogenic attributes and their use in a World Map of Orogens**

527 Due to space and legibility issues, as well as the polycyclic nature of deformation and
528 metamorphism, many orogenic features are difficult to represent on a World Map of Orogens.
529 In order to overcome these constraints, it becomes necessary to identify deformation zones at a
530 regional scale, and to organize them in terms of fundamental components of a “typical”
531 mountain belt. In addition, another issue that requires careful consideration is the
532 spatiotemporal overprint of orogenic events. As outlined in this paper, we have identified key
533 elements of different types of orogens in order to define a number of “typical” orogens and map
534 them on a World map. To do so, we propose the creation of several layers corresponding to
535 time windows that encompass the development of a given orogen. This superposition of these
536 layers allows us to highlight a range of continental growth processes and events through time.
537 Thus, our approach hinges on the identification of a spatial zonation that is common to many
538 (most?) mountain belts and uses geological concepts that are based on the global rock record.
539 The proposed zonation comprises elements that characterize the architecture of many mountain
540 belts and include in the internal zone: lower plate “crystalline” metamorphic complexes (often

541 but not always corresponding to older lithostratigraphic substratum) modified by thick-skin
542 structures and (U)HP and (U)HT metamorphism, overlain by deformed sedimentary rocks
543 deposited in former distal oceanic areas and possibly ophiolitic slivers of oceanic crust. In
544 contrast, the orogenic upper plate usually contains relics of magmatic arcs and associated
545 (U)HT metamorphism formed prior to collision and ophiolites corresponding to associated
546 back-arc and fore-arc basins. The adjacent foreland and hinterland domains are devoid of high
547 grade metamorphic assemblages and are generally dominated by thin-skin structures that
548 deform sedimentary strata (**Table 1**).

549 In this broad view of orogenic architecture, there are of course many additional complexities
550 that can originate with back-thrusting of lithostratigraphic units for example and that result in
551 structurally-complex domains. Nevertheless, common features such as the direction and
552 polarity of convergence as documented with folds, faults and fold-and-thrust belts can be
553 documented globally. Thus, the proposed zonation (early orogenic, orogenic, peri-orogenic and
554 para-orogenic zones) is useful and certainly reflects key geodynamic processes pertinent to the
555 evolution of orogens through time.

556 The use of the four-fold classification of orogens is therefore expected to document the growth
557 and modification of continents through time and space since 2.5 Ga. We propose to distinguish
558 the various deformation zones (and their components) on the World Map of Orogens with
559 different shades of the same color and thus improve our understanding of the evolution of
560 orogens from early Earth geodynamic processes to current plate tectonic dynamics within a
561 continuum of deformation.

562 **7. Conclusion**

563 In the classic Wilson Cycle model, there is a space-time continuum of deformation,
564 during which the various geological elements of a mountain belt system are actively deformed.
565 Since the Wilson Cycle nevertheless treats these elements independently, whereas modern

566 concepts consider the various geodynamic processes to be intimately linked during orogenic
567 evolution, we propose that consideration of the various stages in mountain building may help
568 in the classification of convergent orogens. To a certain extent, this implies considering inherent
569 links between the various compressional stages, which can be either end-member type (i.e. well-
570 defined spatially and temporarily) or transient (i.e. changing in space and time).

571 We consider that orogenic zones, which are characterized by (U)HP metamorphism, (U)HT
572 metamorphism, magmatism (aluminous granites) and/or ophiolites (= orogenic zone in types II
573 and III), represent the core of the orogenic system and correspond to what is often referred to
574 as the “internal zone”. Such zones can be readily documented in the older orogens even though
575 erosion may have removed much of the higher structural level rock record. On the other hand,
576 the peri-orogenic zones, in which deformation includes fold-thrust belts and low-grade
577 metamorphism (= peri-orogenic zones in types II and III and early or para-orogenic zones in
578 types I and IV), may have in part (but generally not completely) been eroded in ancient orogens.
579 These are important elements to take in account to achieve a full understanding of the internal
580 architecture of orogens, as well as their sequencing, history, and role in the growth and
581 reorganization of continents with time.

582 **8. Acknowledgments**

583 This paper is the result of collaborative discussions within the framework of IGCP
584 project 667. The project is funded by IUGS via UNESCO and we thank these organizations for
585 their support. We also thank the CGMW for the support provided by their staff and for the
586 organization of meetings. The RMCA is acknowledged for the organization of the 2019 annual
587 meeting in Belgium, Romain Bousquet (Kiel University) for his precious help and his many
588 suggestions for the figures, Solen Le Gardien (SGF) for her help with the references and
589 Benjamin Sautter for his benevolent proofreading. The IGCP667 team is a large group and the
590 name of all the participants can be found with the following link: [CGMW/IGCP667](https://www.cgmw.org/IGCP667)

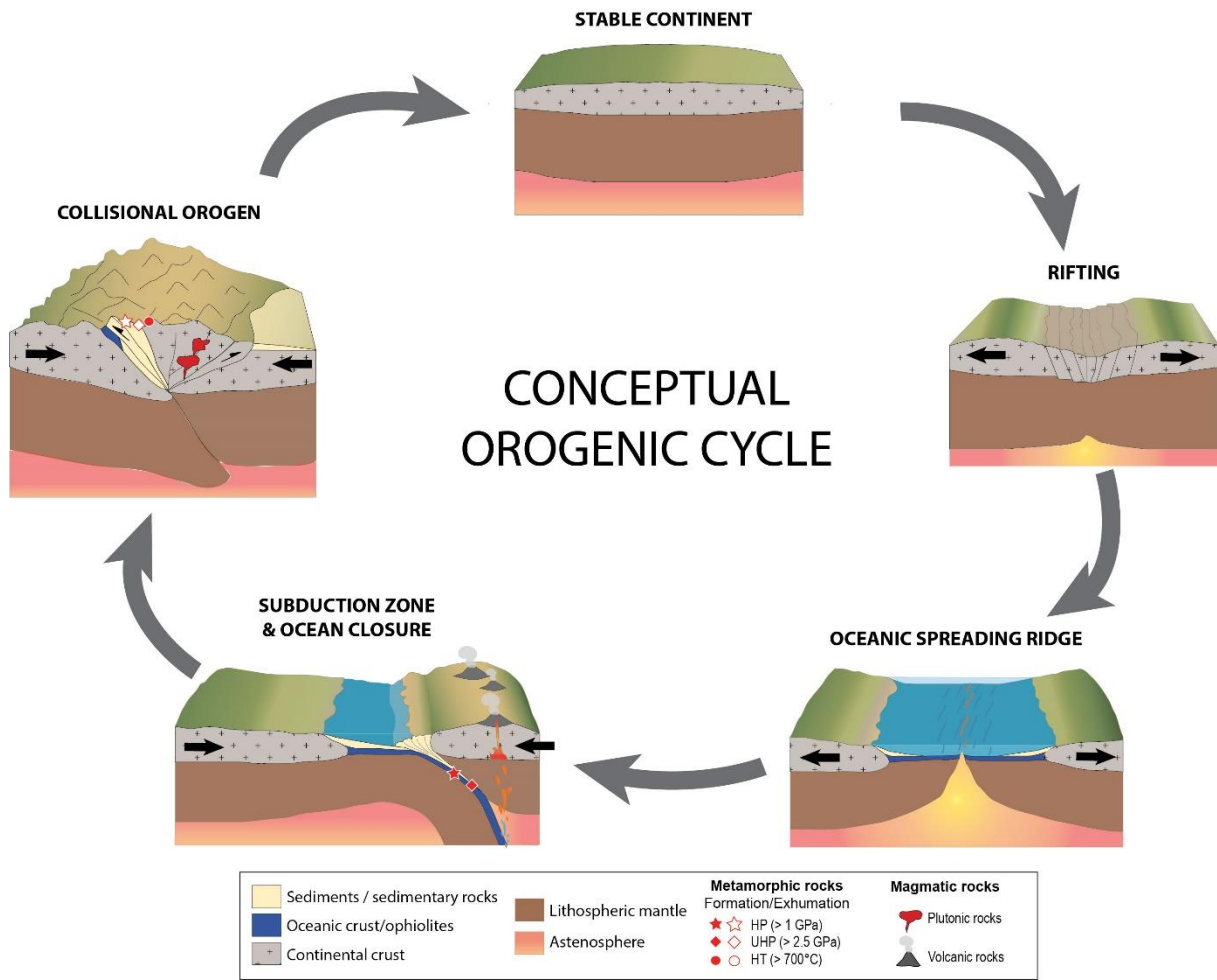
591 (<https://ccgm.org/en/content/11-team>). We thank the reviewers for their comments, which
592 improved the content and clarity of the paper greatly. This is Earth Sciences Sector contribution
593 #xxxx.

594 **9. Captions**

595 *Table 1. Relevant geodynamic components and attributes by orogenic zones*

Types of orogens	Orogenic zones	Oceanic closure	Magmatism	Metamorphism	Fold and Thrust Belt	Pre- to syn-orogenic sediment deposit	Late- to post orogenic sediment deposit
Cordilleras (Type I)	EARLY-OROGENIC	in progress	Volcanic & plutonic rocks (Primary melts, dominantly calco-alkaline)	in lower part: HP/LT	Accretionary prism	Formation of a retro-arc foreland basin, Thick sedimentary sequence Flysch-Accretionary wedge	Absent but sediments deposited in the forearc basin may unconformably cover the FTB
Accreted terranes (Type II)	OROGENIC	YES (Multiple) ophiolites	Syn-collisional (Migmatites and aluminous granites)	(U)HP (U)HT	-	-	-
	PERI-OROGENIC	-	-	-	FTBs form where passive continental margins collide with a subduction zone	-	Molassic basin
Continent-Continent (Type III)	OROGENIC	YES ophiolites or ophiolitic mélange	Syn-collisional (Migmatites and (per)-aluminous granites)	HP/UHP (prograde) during continental subduction and MP-LP/(U)HT (retrograde) coeval with crustal melting	-	Passive continental margin deposits	-
	PERI-OROGENIC	-	-	-	Bilateral foreland/hinterland FTB	Passive continental margin deposits, (volcanic)-sedimentary terrigenous rocks turbiditic deposits	Thick molassic deposits in foreland and hinterland basins. Intramontane basins

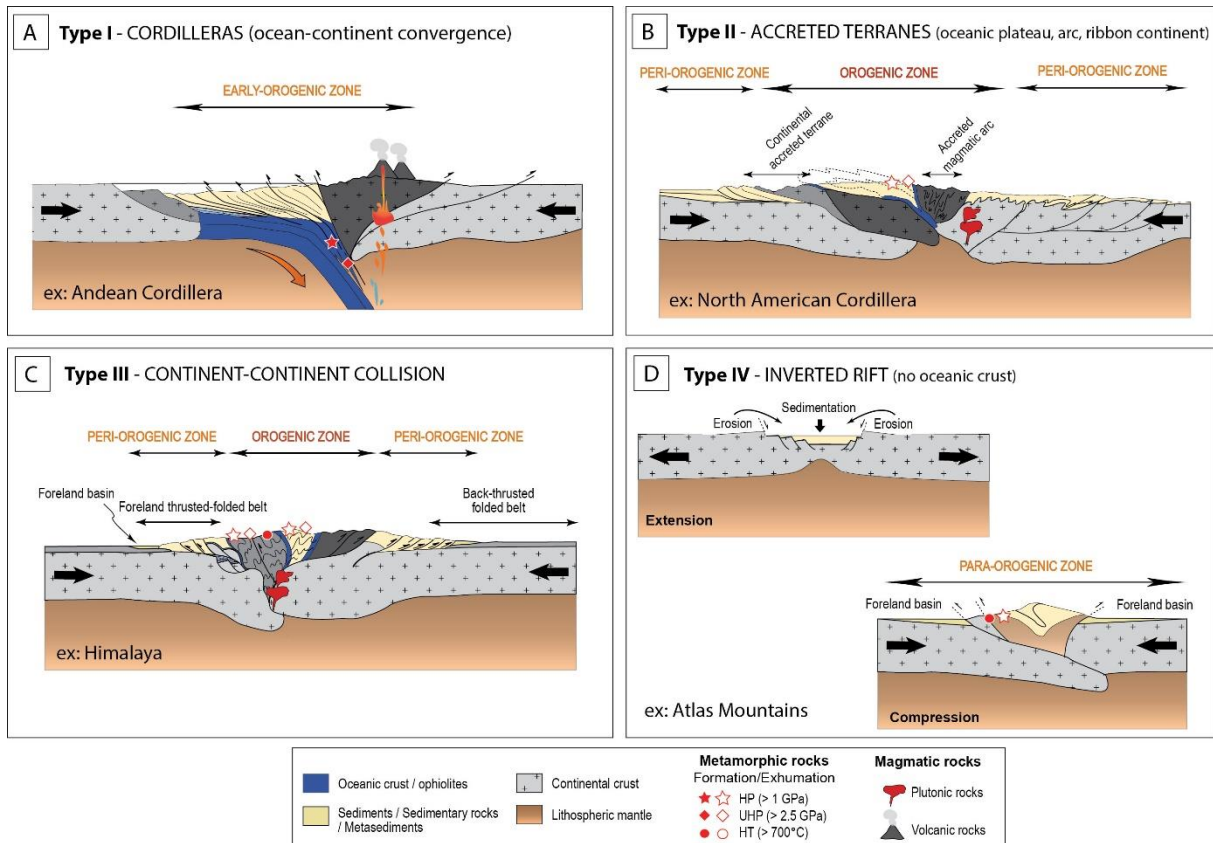
Inverted rift (Type IV)	INTRAPLATE / PARA- OROGENIC	NO real oceanic closure	No magmatic arc Migmatites and (per)aluminous granites	Prograde and retrograde metamorphism	FTB	Passive continental margin deposits, (volcanic)-sedimentary terrigenous rocks	Molassic deposit
------------------------------------	-----------------------------------	-------------------------------	---	--	-----	--	------------------



598

599 **Fig.1.** Cyclic view of the different stages of a theoretical orogenic cycle as an extension-
 600 compression continuum (Wilson Cycle). The uplift, erosion and unroofing processes including
 601 exhumation of metamorphosed rocks and crustal melting occur in the transition between the
 602 collisional orogen stage and the stable continent stage.

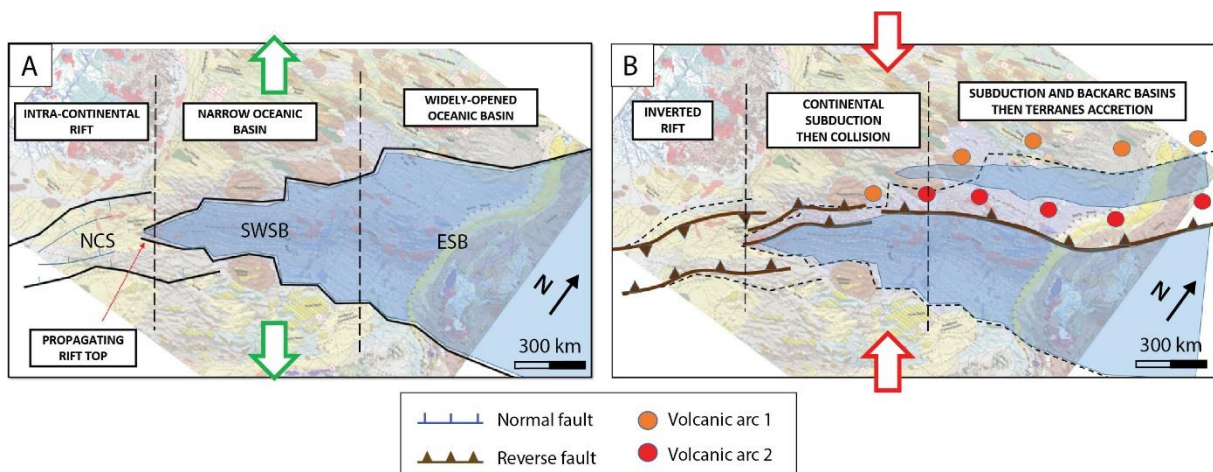
603



604

605 **Fig.2.** The different types of orogens. (a) Subduction type, (b) accreted terranes type, (c)
 606 continental collision type (d) intracontinental type. Figures modified from *Lagabrielle and*
 607 *Bodinier, 2008; Robert and Bousquet, 2018.*

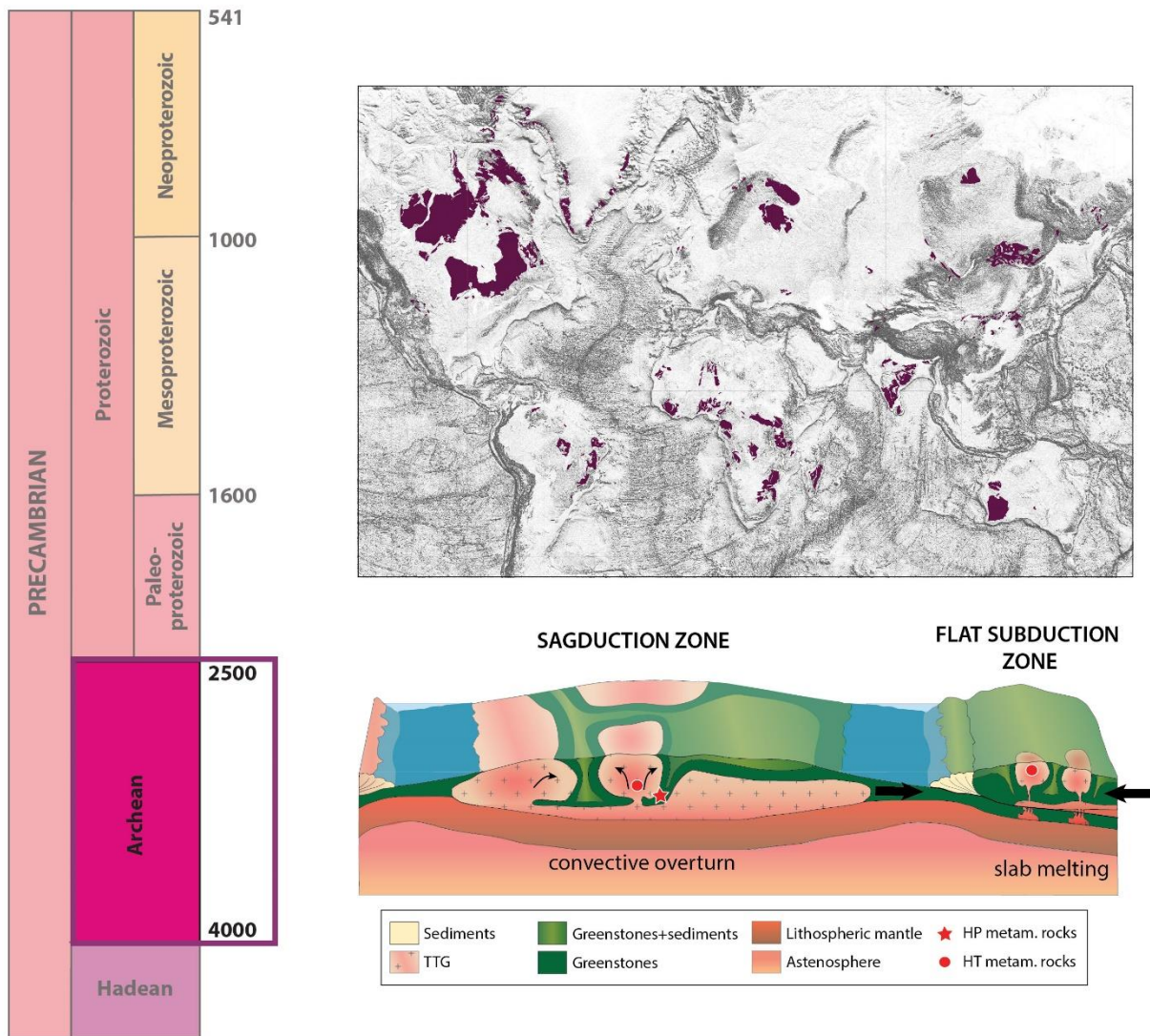
608



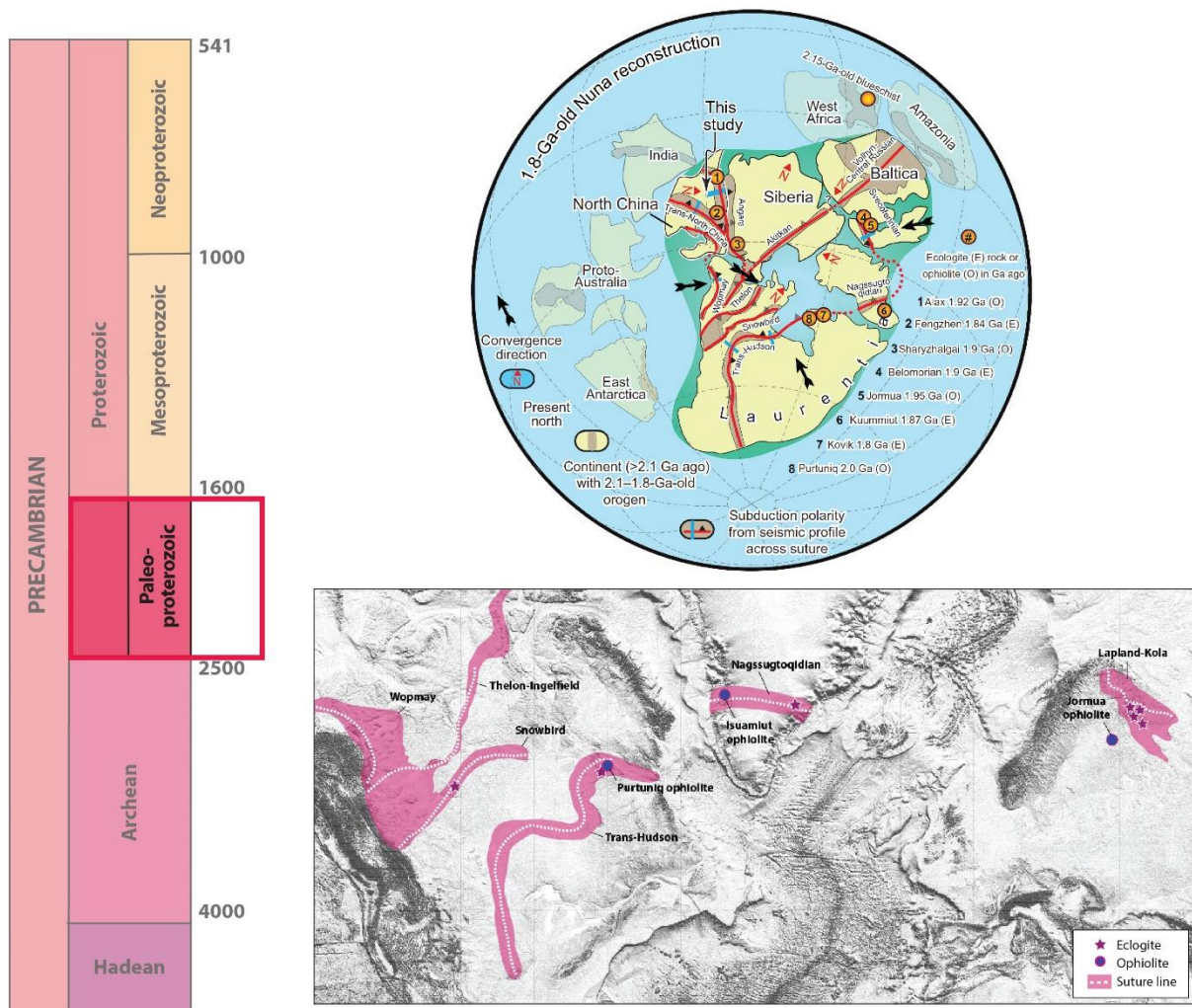
609

610 **Fig.3.** Theoretical “scissor shape”. (a) Active opening setting and (b) projected setting during
 611 shortening. The background is an example modified from *Pubellier et al., 2016; NCS; Nam*

612 Con Son Basin, SWSB; SW sub-basin, ESB; Eastern Sub-basin. Figure (b) is a speculative
 613 scenario for future basin closure.
 614



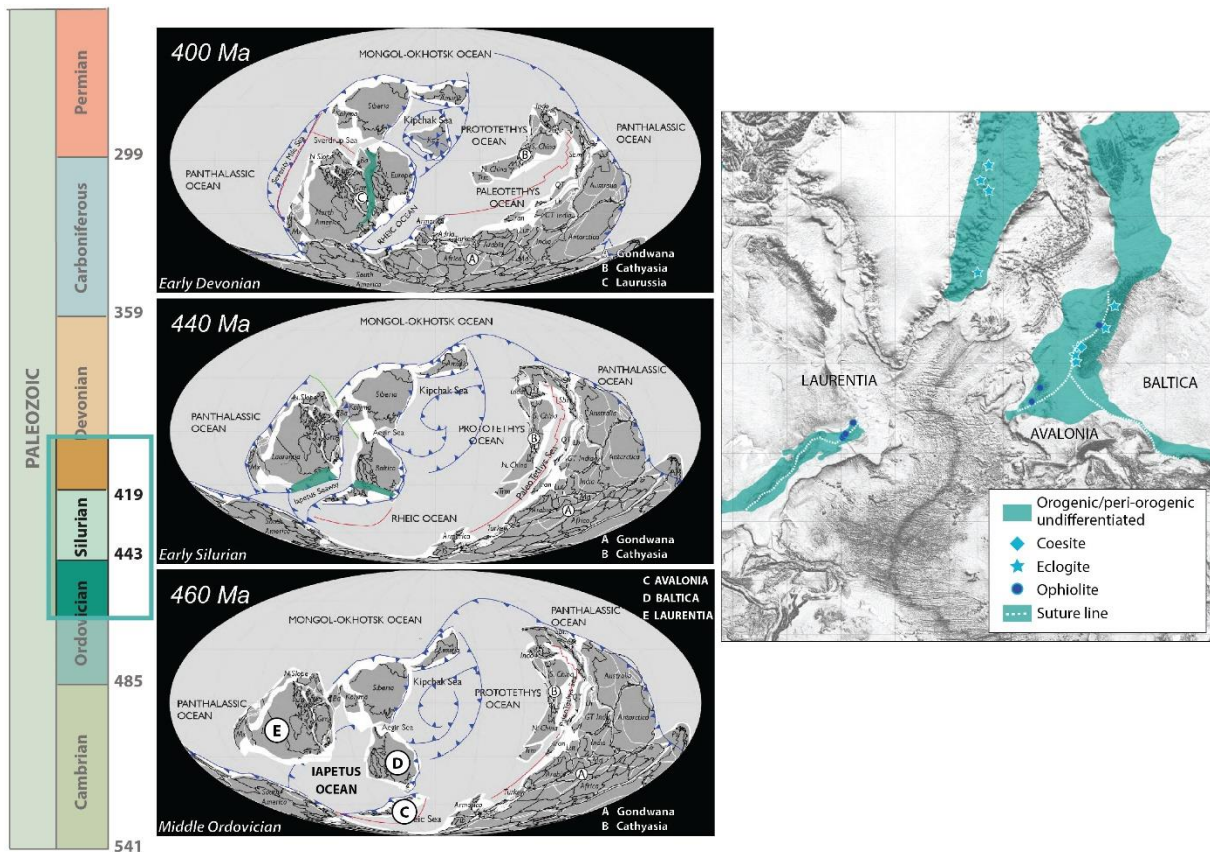
615
 616 **Fig.4.** Extent of Archean crust on the World Map and representative Archean dome and keel
 617 structures formed by geodynamical processes that ended at about 2.5 Ga: flat subduction and
 618 sagduction of dense greenstone lithologies into lighter felsic crystalline basement. The higher
 619 mantle heat flux is envisioned as leading to the partial melting of the lower crust (flat
 620 subduction) and the convective overturn of the Archean crust (sagduction).
 621



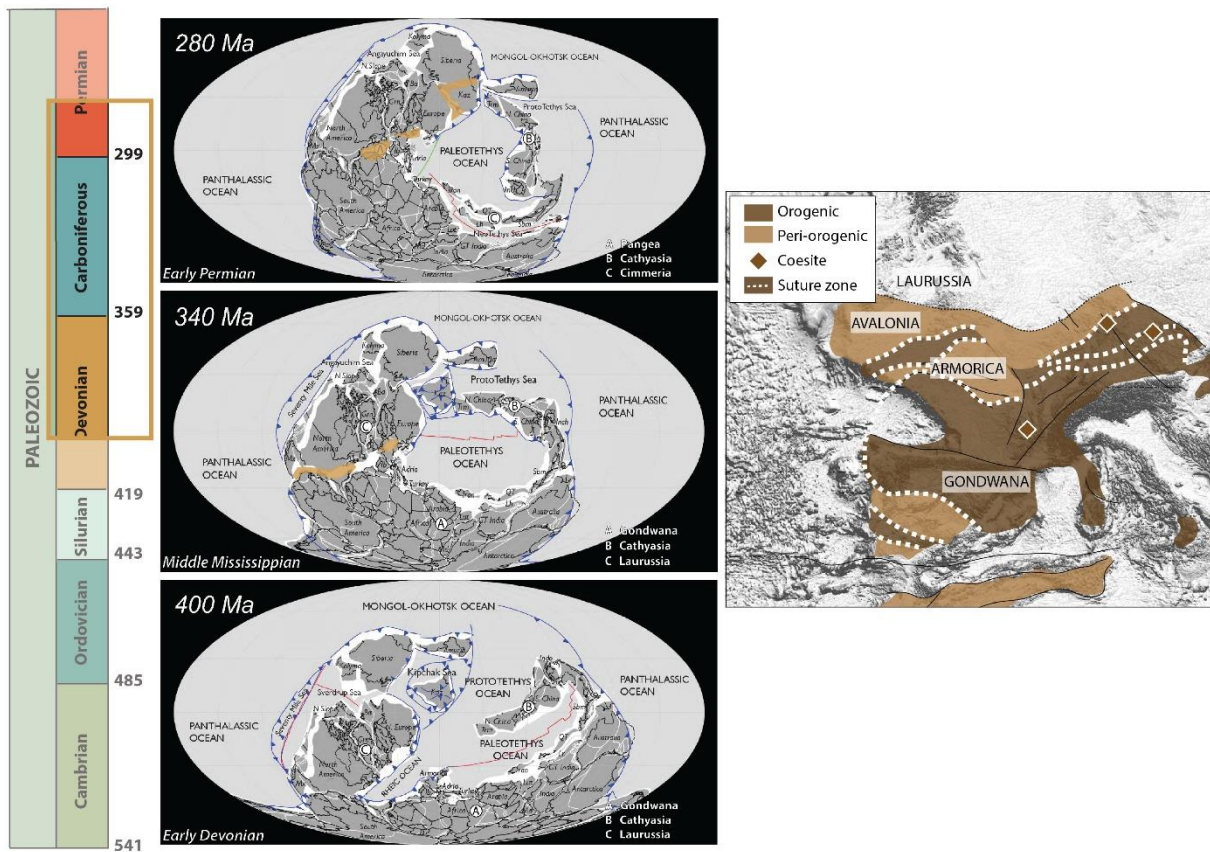
622

623 **Fig.5.** Present extent of some of the Paleoproterozoic orogens (may include reworked Archean
 624 crust) in the North Atlantic realm on the World Map, and in the past as shown on a Nuna
 625 reconstruction ~1.8 Ga ago (*Evans and Mitchell, 2011*), including the position of North China
 626 (*Wan et al., 2020*). Convergence directions (black arrows) are inferred from subduction polarity
 627 (black triangles) indicated at seismic profiles (blue). Speculated continuation of seismically
 628 confirmed sutures (red). A 2.15-Ga-old blueschist immediately preceding the Orosirian period
 629 is shown (*Ganne et al., 2012*). Green region marks configuration of core continents assembled
 630 through two to three major sutures. Putative positions in the larger supercontinent Nuna are
 631 suggested for other less studied continents (slightly transparent). Seismic evidence is consistent
 632 with previous paleomagnetic and geological configurations in the green region under the
 633 paradigm of a modern, global subduction-driven plate tectonic network. From *Wan et al.*

634 (2020). Location of eclogites and blueschist from: Kola-Lapland orogen, Belomorian Province,
 635 Russia (Volodichev et al., 2004; Skublov et al., 2011; Slabunov et al., 2011); Nagssugtoqidian
 636 orogen, South-East Greenland (Nutman et al., 2008; Müller et al., 2018); Trans-Hudson orogen,
 637 North America (Weller & St-Onge, 2017); Snowbird Tectonic Zone, Canada (Snoeyenbos et
 638 al., 1995; Baldwin et al., 2003; 2004).

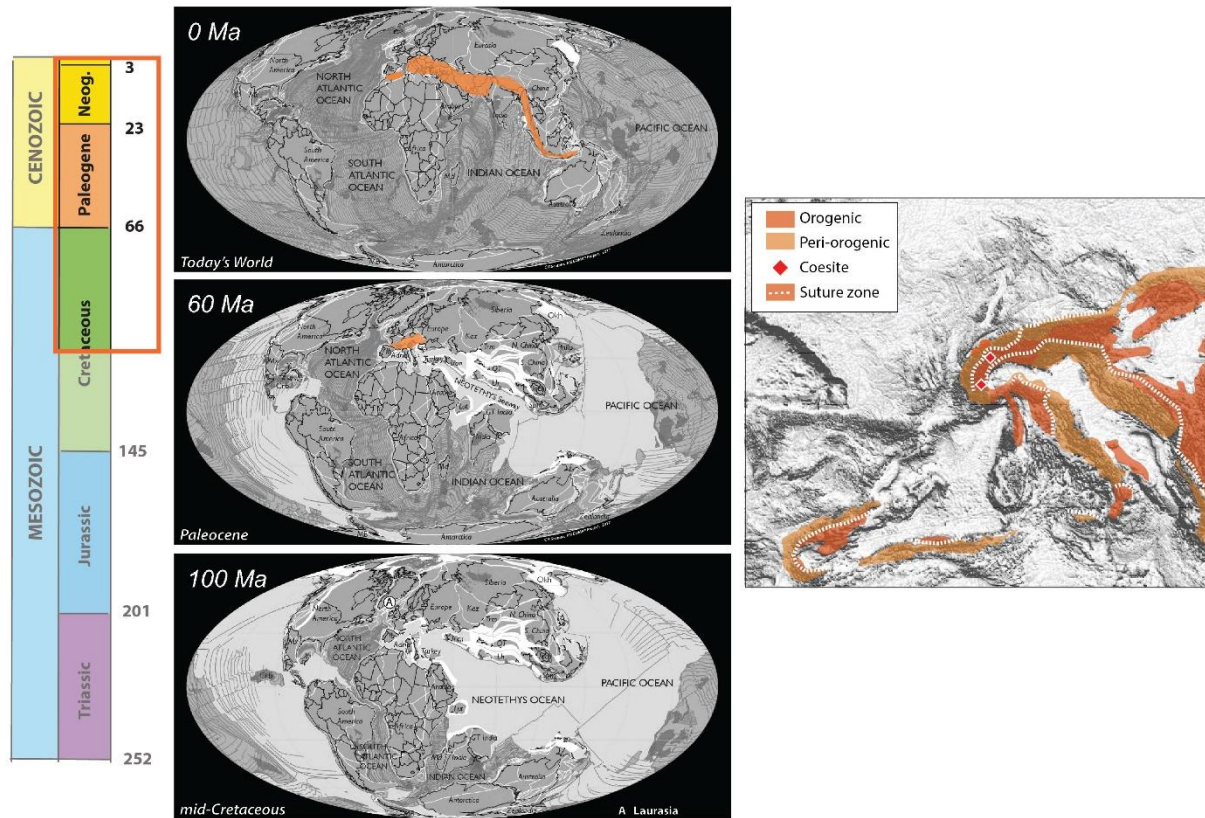


639
 640 **Fig.6.** Present location of the Caledonian orogen resulting from the progressive closure of the
 641 Iapetus Ocean shown on the World Map and in the past as shown on paleogeographic
 642 reconstructions from Scotese, *PALEOMAP Project* (www.scotese.com).



643

644 **Fig.7.** Present location of the Variscan orogens shown on the World Map and in the past as
 645 shown on paleogeographic reconstructions from Scotese, *PALEOMAP Project*
 646 (www.scotese.com).



647

648 **Fig.8.** (a) Present location of the Alpine orogens (following closure of the Neo-Tethys and
 649 Alpine oceans) shown on the World Map and in the past as shown on paleogeographic
 650 reconstructions from Scotese, *PALEOMAP Project* (www.scotese.com).

651 10. References

652 Abbott, D. H., Hoffman, S. E., 1984. Archaean plate tectonics revisited 1. Heat flow, spreading
 653 rate, and the age of subducting oceanic lithosphere and their effects on the origin and evolution
 654 of continents. *Tectonics* 3 (4), 429–448.

655 Abbott, D., Burgess, L., Longhi, J., Smith, W. H. F. 1994. An empirical thermal history of the
 656 Earth's upper mantle. *J. Geophys. Res.* 99 (B7), 13835–13850.

657 Abu Sharib, A.S.A.A., Maurice, A.E., Abd El-Rahman, Y.M., Sanislav, I.V., Schulz, B.,
 658 Bakhit, B.R., 2019. Neoproterozoic arc sedimentation, metamorphism and collision: Evidence
 659 from the northern tip of the Arabian-Nubian Shield and implication for the terminal collision
 660 between East and West Gondwana. *Gondwana Research*, 66, 13–42.

661 Arndt, N. T., Nisbet, E. G., 1982. *Komatiites*. Taylor and Francis.

662 Baldwin, J. A., Bowring, S. A., & Williams, M. L., 2003. Petrological and geochronological
 663 constraints on high pressure, high temperature metamorphism in the Snowbird tectonic zone,
 664 Canada. *Journal of Metamorphic Geology*, 21(1), 81-98.

665 Baldwin, J. A., Bowring, S. A., Williams, M. L. and Williams, I. S. 2004. Eclogites of the
 666 Snowbird tectonic zone: petrological and U-Pb geochronological evidence for Paleoproterozoic

667 high-pressure metamorphism in the western Canadian Shield. *Contrib. Mineral. Petrol.* 147(5),
668 528–548).

669 Ballèvre, M., Bosse, V., Ducassou, C., Pitra, P., 2009. Palaeozoic history of the Armorican
670 Massif: Models for the tectonic evolution of the suture zones. *C. R. Geoscience* 341, 174-201.

671 Barrier, E. and Vrielynck, B. 2008. Atlas MEBE - Palaeotectonic Maps of the Middle East
672 (Middle East Basins Evolution Programme). CCGM.org

673 Bastow, I.D., Thompson, D.A., Wookey, J., Kendall, J-M., Helffrich, G., Snyder, D.B., Eaton,
674 D.W., and Darbyshire, F.A., 2011. Precambrian plate tectonics: seismic evidence from northern
675 Hudson Bay, Canada. *Geology*. 39, 91–94.

676 Beauchamp W., Allmendinger R. W., Barazangi M., Demnati A., El Alji M., Dahmani M. 1999.
677 Inversion tectonic and the evolution of the High Atlas mountains, Morocco, based on a
678 geological-geophysical transect. *Tectonics* 18, 163-184.

679 Beaumont, C, Kamp, P. J. J., Hamilton J. and Fullsack P. 1996. The continental collision zone,
680 South Island, New Zealand. Comparison of geodynamical models and observations. *J.*
681 *Geophys. Res.* 101, B2, 3333-3359. doi.org/10.1029/95JB02401

682 Bédard JH, Harris LB, Thurston PC., 2013. The hunting of the snArc. *Precambrian Res.*
683 229:20–48

684 Bédard, JH., 2018. Stagnant lids and mantle overturns: implications for Archaean tectonics,
685 magmagenesis, crustal growth, mantle evolution, and the start of plate tectonics. *Geosci. Front.*
686 9:19–49

687 Block: key observations and controversies. *Gondwana Res.* 23, 1273–1305.

688 Boniface, N., Schenk, V. and Appel, P. 2012. Paleoproterozoic eclogites of MORB-type
689 chemistry and three Proterozoic orogenic cycles in the Ubendian Belt (Tanzania): Evidence
690 from monazite and zircon geochronology, and geochemistry. *Precamb. Res.* 192, 16–33.

691 Bousquet R, Goffé. B, Wiederkehr M, Koller F, Schmid SM, Schuster R, Engi M, Martinotti
692 G. 2008. Metamorphism of metasediments at the scale of an orogen: a key to the Tertiary
693 geodynamic evolution of the Alps. *Geol Soc Lond Spec Publ* 298:393–411

694 Briais, A., Patriat, P. and Tapponnier, P., 1993. Updated interpretation of magnetic anomalies
695 and seafloor spreading stages in the South China Sea: Implications for the Tertiary tectonics of
696 Southeast Asia. *Journal of Geophysical Research: Solid Earth*, 98(B4), 6299-6328.

697 Brown, D. A., Tamblyn, R., Hand, M., & Morrissey, L. J., 2020. Thermobarometric constraints
698 on burial and exhumation of 2-billion-year-old eclogites and their metapelitic
699 hosts. *Precambrian Research*, 347, 105833.

700 Brown, M. 2008. Characteristic thermal regimes of plate tectonics and their metamorphic
701 imprint throughout Earth history: When did Earth first adopt a plate tectonics mode of behavior?
702 *When Did Plate Tectonics Begin on Planet Earth?* 440, 97.

703 Brown, M. and Johnson, T. E. 2018. Invited Centennial Article: Secular change in
704 metamorphism and the onset of global plate tectonics. *Am. Mineral.* 103, 181-196.

705 Bulois, C., Pubellier, M., Chamot-Rooke, N., Delescluse, M. 2018. Successive rifting events in
706 marginal basins: the example of the Coral Sea region (Papua New Guinea), 2017. *Tectonics*,
707 Volume 37, Issue 1, 3-29. DOI10.1002/2017TC004783

- 708 Charvet J., Shu L.S. Faure M., Choulet, F., Wang, B., Le Breton N., 2010. Structural
709 development of the Lower paleozoic belt of South China : genesis of an intracontinental orogen.
710 *J. of Asian Earth Sci.*, 39, 309-330.
- 711 Chen K, Rudnick RL, Wang Z, Tang M, Gaschnig RM, et al., 2019. How mafic was the Archean
712 upper continental crust? Insights from Cu and Ag in ancient glacial diamictites. *Geochim.*
713 *Cosmochim. Acta.* <https://doi.org/10.1016/j.gca.2019.08.002>
- 714 Chen, L., Huang, B., Yi, Z. , Zhao, J., Yan, Y., 2013. Paleomagnetism of ca. 1.35 Ga sills in
715 northern North China Craton and implications for paleogeographic reconstruction of the
716 Mesoproterozoic supercontinent. *Precambrian Res.* 228, 36–47.
- 717 Choulet F., Faure M., Cluzel, Chen Y., Lin W., Wang B., Jahn B-M. 2012. Architecture and
718 Evolution of Accretionary Orogens in the Altaids Collage: The Early Paleozoic West Junggar
719 (NW China). *American Journal of Science*, 312, 1098-1145.
- 720 Clift, P., Lin, J., and Barckhausen, U. 2002, Evidence of low flexural rigidity and low viscosity
721 lower continental crust during continental break-up in the South China Sea: *Marine and*
722 *Petroleum Geology*, v. 19, no. 8, p. 951-970.
- 723 Cocks, L. R. M, and Torsvik, T. H. 2006. European geography in a global context from the
724 Vendian to the end of the Palaeozoic. In Gee, D. G. and Stpenson, R. A. (eds). *European*
725 *Lithosphere Dynamics*. Geological Society, London, *Memoirs*, 32, 83–95.
- 726 Collins, A. S., Reddy, S. M., Buchan, C. and Mruma, A. 2004. Temporal constraints on
727 Palaeoproterozoic eclogite formation and exhumation (Usagaran Orogen, Tanzania). *Earth*
728 *Planet. Sci. Lett.* 224(1), 175-192.
- 729 Collins, W. J., Van Kranendonk, M. J., Teyssier, C., 1998. Partial convective overturn of
730 Archaean crust in the east Pilbara Craton, Western Australia: driving mechanisms and tectonic
731 implications. *J. Struct. Geol.* 20 (9), 1405-1424.
- 732 Coltice, N., Bertrand, H., Rey, P., Jourdan, F., Phillips, B. R., Ricard, Y., 2009. Global warming
733 of the mantle beneath continents back to the Archaean. *Gondwana Res.* 15 (3), 254-266.
- 734 Coney, P., Jones, D. and Monger, J. 1980. Cordilleran suspect terranes. *Nature* 288, 329-333
735 <https://doi.org/10.1038/288329a0>
- 736 Connelly, J.N., Thrane, K., Krawiec, A.W., and Garde, A.A., 2006. Linking the
737 Palaeoproterozoic Nagssugtoqidian and Rinkian orogens through the Disko Bugt region of
738 West Greenland. *Journal of the Geological Society, London.* 163, 319–335.
- 739 Corrigan, D., 2012. Paleoproterozoic crustal evolution and tectonic processes: Insight from the
740 LITHOPROBE program in the Trans-Hudson orogeny, Canada: in Percival, J.A., Cook, F.,
741 Clowes, R., eds., *Tectonic Styles in Canada: The LITHOPROBE Perspective*. Geological
742 Association of Canada, *Special Paper* 49, 237–284.
- 743 Corrigan, D., Pehrsson, S., Wodicka, N., and de Kemp, E., 2009. The Palaeoproterozoic Trans-
744 Hudson orogen: a prototype of modern accretionary processes. *Geological Society, London,*
745 *Special Publication* 327, 457–479.
- 746 Courtillot, V., 1982, *Propagating rifts and continental breakup Tectonics*, Volume 1, Issue 3.
747 Doi: 10.1029/TC001i003p00239
- 748 d'Acromont, E., Leroy, S., Maia, M., Patriat, P., Beslier, M. O., et al. 2006. Structure and
749 evolution of the eastern Gulf of Aden: insights from magnetic and gravity data (Encens-Sheba

- 750 MD117 cruise). *Geophysical Journal International*, Oxford University Press (OUP), 165 (3),
751 pp.786-803. doi:10.1111/j.1365-246X.2006.02950.x
- 752 Daly, J.S., Balagansky, V.V., Timmerman, M.J., and Whitehouse, M.J., 2006. The Lapland-
753 Kola orogen: Palaeoproterozoic collision and accretion of the northern Fennoscandian
754 lithosphere. *Geological Society, London, Memoirs*, 32, 579–598.
- 755 Dana, J.D., 1873. On some results of the Earth's contraction from cooling, including a
756 discussion of the origin of mountains and the nature of the Earth's interior. Part I *Am. Jour.*
757 *Sci.*, ser 3, v. 5, art 46. 423-443.
- 758 de Oliveira Chaves, A., and Porcher, C.C., 2020. Petrology, geochemistry and Sm-Nd
759 systematics of the Paleoproterozoic Itaguara retroeclogite from São Francisco/Congo Craton:
760 One of the oldest records of the modern-style plate tectonics. *Gondwana Research*, 87, 224–
761 237.
- 762 de Oliveira Chaves, A., and Porcher, C. C. 2020. Petrology, geochemistry and Sm-Nd
763 systematics of the Paleoproterozoic Itaguara retroeclogite from São Francisco/Congo Craton:
764 One of the oldest records of the modern-style plate tectonics. *Gondwana Research*, 87, 224-
765 237.
- 766 Ding, W. and Li, J., 2016. Propagated rifting in the Southwest Sub-basin, South China Sea:
767 Insights from analogue modelling. *Journal of Geodynamics*, 100, pp.71-86.
- 768 Dumond, G., 2020. Tibetan dichotomy exposed in the Canadian Shield: A lower crustal
769 perspective. *Earth and Planetary Science Letters*, 544, 116375.
- 770 Eaton, D.W., and Darbyshire, F., 2010. Lithospheric architecture and tectonic evolution of the
771 Hudson Bay region. *Tectonophysics*, 480, 1–22.
- 772 Elie de Beaumont, M.L., 1852. *Notice sur les systèmes des Montagnes*. 3 vol. Paris. 1543 pp.
- 773 Evans, D. A. D., Mitchell, R. N., 2011. Assembly and breakup of the core of Paleoproterozoic–
774 Mesoproterozoic supercontinent Nuna. *Geology* 39, 443–446.
- 775 Evans, D.A.D., and Mitchell, R.N., 2011. Assembly and breakup of the core of
776 Paleoproterozoic-Mesoproterozoic supercontinent Nuna. *Geology*, 39, 443–446.
- 777 Evans, D.A.D., Veselovsky, R.V., Petrov, P.Y, Shatsillo, A.V., and Pavlov, V.E., 2016.
778 Paleomagnetism of Mesoproterozoic margins of the Anabar Shield: A hypothesized billion-
779 year partnership of Siberia and northern Laurentia. *Precambrian Research*, 281, 639–655.
- 780 Faill, R. T. (1997). A geologic history of the north-central Appalachians; Part 1, Orogenesis
781 from the Mesoproterozoic through the Taconic Orogeny. *American Journal of Science*, 297(6),
782 551-619.
- 783 Faure M., Bé Mézème E., Cocherie A., Rossi P., Chemenda A., Boutelier D. 2008, Devonian
784 geodynamic evolution of the Variscan Belt, insights from the French Massif Central and Massif
785 Armoricaïn, *Tectonics*, 27, TC2008, <http://dx.doi.org/10.1029/2007TC002115>.
- 786 Faure M., Be Mézème E., Duguet M., Cartier C., Talbot J-Y. 2005. Paleozoic tectonic evolution
787 of medio-Europa from the example of the French Massif Central and Massif Armoricaïn. In: R.
788 Carosi et al. (eds). *Journal of the Virtual Explorer*, ISSN 1441-8142, Volume 19, Paper 5.
789 doi:10.3809/jvirtex. 2005. 00120

- 790 Faure M., Shu LS., Wang,B., Charvet J., Choulet F., Monié P. 2009. Intracontinental
791 subduction: a possible mechanism for the Early Palaeozoic Orogen of SE China. *Terra Nova*,
792 21, 360-368.
- 793 Faure, M., Nguyen V.V., Hoai, L.T.T., Lepvrier, C., 2018. Early Paleozoic or Early-Middle
794 Triassic collision between the South China and Indochina Blocks: the controversy resolved?
795 Structural insights from the Kon Tum massif (Central Vietnam). *J.A.E.S.* 166, 162-180.
796 doi.org/10.1016/j.jseaes.2018.07.015.
- 797 Fournier, M., Chamot-Rooke, N., Petit, C., Huchon P., Al-Kathiri, A., Audin, L., Beslier, M.-
798 O., d'Acremont, E., Fabbri, O., Fleury, J.-M., Khanbari, K., Lepvrier, C., Leroy, S., Maillot,
799 B., and Merkouriev, S. 2010, Arabia-Somalia plate kinematics, evolution of the Aden-Owen-
800 Carlsberg triple junction, and opening of the Gulf of Aden, *J. Geophys. Res.*, 115, B04102,
801 DOI: 10.1029/2008JB006257
- 802 François, C., Debaille, V., Paquette, J. L., Baudet, D., & Javaux, E. J., 2018. The earliest
803 evidence for modern-style plate tectonics recorded by HP–LT metamorphism in the
804 Paleoproterozoic of the Democratic Republic of the Congo. *Scientific reports*, 8(1), 1-10.
- 805 François, C., Philippot, P., Rey, P. and Rubatto, D. 2014. Burial and exhumation during
806 Archean sagduction in the east Pilbara granite greenstone terrane. *Earth Planet. Sci. Lett.* 396,
807 235–251.
- 808 Frizon de Lamotte, D., Saint Bézar, B., Bracène, R., Mercier, E. 2000. The two main steps of
809 the Atlas building and geodynamics of the western Mediterranean, *Tectonics* 19,740-761.
- 810 Ganne, J., De Andrade, V., Weinberg, R. F., Vidal, O., Dubacq, B., Kagambega, N., Naba, S.,
811 Baratoux, L., Jessell, M., Allibon, J., 2012. Modern-style plate subduction preserved in the
812 Palaeoproterozoic West African craton. *Nat. Geosci.* 5, 60–65.
- 813 Gapais D, Cagnard F, Gueydan F, Barbey P, Ballèvre M., 2009. Mountain building and
814 exhumation processes through time: inferences from nature and models. *Terra Nova* 21:188–
815 94
- 816 Garde, A.A.,and Hollis, J.A., 2010. A buried Palaeoproterozoic spreading ridge in the northern
817 Nagssugtoqidian orogen, West Greenland. *Geological Society, London, Special Publications*,
818 338, 213–234.
- 819 Grabau, A., 1924. Stratigraphy of China, part I, Paleozoic and older, *Geol. Surv. of Agric. and*
820 *Commerce. Peking.*
- 821 Gressly, A. 1840. Observations géologiques sur le Jura Soleurois: *Allgem. Schweiz. Ges. f.d.*
822 *ges. Naturw., Neue Denkschr*, 4, 115-241.
- 823 Handy, M., R., Schmid, S. M, Bousquet, R., Kissling, E., Bernoulli, D. 2010. Reconciling plate-
824 tectonic reconstructions of Alpine Tethys with the geological–geophysical record of spreading
825 and subduction in the Alps. *Earth-Science Reviews* 102, 121-158. doi:
826 10.1016/j.earscirev.2010.06.002.
- 827 Handy, M., R., Ustaszewski, K., and Kissling, E. 2014. Reconstructing the Alps–Carpathians-
828 Dinarides as a key to understanding switches in subduction polarity, slab gaps and surface
829 motion. *Int J Earth Sci (Geol Rundsch)*, 104 (1), 1-26. doi; 10.1007/s00531-014-1060-3.

- 830 Hernández-Montenegro, J. D., Palin, R. M., Zuluaga, C. A., & Hernández-Urbe, D. 2021.
831 Archean continental crust formed by magma hybridization and voluminous partial
832 melting. *Scientific Reports*, 11, Art-5263.
- 833 Hoffman, P.F., 1988. United Plates of America, the birth of a craton: Early Proterozoic
834 assembly and growth of Laurentia. *Annual Review of Earth and Planetary Sciences*, 16, 543–
835 603.
- 836 Hoffman, P.F., 1997. Tectonic genealogy of North America, in van der Pluijm, B.A., Marshak,
837 S., eds., *Earth Structure. An Introduction to Structural Geology and Tectonics*: McGraw-Hill,
838 New York, 459–464.
- 839 Howell, David G., 1989, *Tectonics of Suspect Terranes: Mountain Building and Continental*
840 *Growth*, Eds : Chapman and Hall, 1989, ISBN 10 : 0412303701 ISBN 13 :
841 9780412303708 Hutchison, C. 2005. *Geology of North-West Borneo: Sarawak, Brunei and*
842 *Sabah*: Elsevier, Amsterdam, 448 pp
- 843 Jammes, S., Manatschal, G., Lavier, L., Masini, E. 2009 Tectonosedimentary evolution related
844 to extreme crustal thinning ahead of a propagating ocean: Example of the western Pyrenees,
845 *Tectonics*, Vol 28, 4, 2009
- 846 Jaupart, C., Labrosse, S., Mareschal, J. C. 2007. Temperatures, heat and energy in the mantle
847 of the Earth. In: *Treatise on Geophysics*, vol. 7, pp. 253-303.
- 848 Kearey, P. 1993. Orogeny in: Kearey, P. *The Encyclopedia of the Solid Earth*, p 443-444.
849 Blackwell, 713 pp.
- 850 Kolb, J., 2014. Structure of the Palaeoproterozoic Nagssugtoqidian Orogen, South-East
851 Greenland: Model for the tectonic evolution. *Precambrian Research*, 255, 809–822.
- 852 Korja, A., Lahtinen, R., and Nironen, M., 2006. The Svecofennian orogen: a collage of
853 microcontinents and island arcs. *Geological Society, London, Memoirs*, 32, 561–578.
- 854 Lagabrielle, Y., and Bodinier, J. L. 2008. Submarine reworking of exhumed subcontinental
855 mantle rocks: field evidence from the Lherz peridotites, French Pyrenees. *Terra Nova*, 20(1),
856 11-21.
- 857 Lahtinen, R., Garde, A.A., and Melezhik, V.A., 2008. Paleoproterozoic evolution of
858 Fennoscandia and Greenland. *Episodes*, 31, 1–9.
- 859 Lahtinen, R., and Huhma, H. 2019. A revised geodynamic model for the Lapland-Kola
860 orogen. *Precambrian Research*, 330, 1-19.
- 861 Lardeaux JM., Schulmann K., Faure M., Janousek V., Lexa O., Skrzypek E., Edel J-B., Stipska
862 P., 2014. The Moldanubian Zone in French Massif Central, Vosges/Schwarzwald and
863 Bohemian Massif revisited: Differences and similarities. In « *The Variscan Orogeny: Extent,*
864 *Timescale and the Formation of the European Crust* ». Schulmann, K. et al. (eds). *Geological*
865 *Society, London, Special Publications*, 405, [http://dx.doi.org/10.1144/ SP405.14](http://dx.doi.org/10.1144/SP405.14)
- 866 Lesley, J. P. cited in Chamberlin, T. C., & Salisbury, R. D., 1906. *Geology*, Vol. II. Chicago,
867 p.125.
- 868 Lewry, J., and Stauffer, M., 1990. The Early Proterozoic Trans-Hudson Orogen of North
869 America. *Geological Association of Canada, Special Paper*, 37.

- 870 Li, L., Clift, P. D., Stephenson, R., and Nguyen, H. T., 2014. Non-Uniform Hyper-Extension
871 in Advance of Seafloor Spreading on the Vietnam Continental Margin and the SW South China
872 Sea: Basin Research, no. 26, p. 106-134. doi: 10.1111/bre.12045.
- 873 Li, Z. X., Li, X. H., Wartho, J. A., Clark, C., Li, W. X., Zhang, C. L., & Bao, C. (2010).
874 Magmatic and metamorphic events during the early Paleozoic Wuyi–Yunkai orogeny,
875 southeastern South China: New age constraints and pressure- temperature conditions.
876 Geological Society of America Bulletin, 122, 772–793.
- 877 Loose, D. and Schenk, V. 2018. 2.09 Ga old eclogites in the Eburnian-Transamazonian orogen
878 of southern Cameroon: Significance for Palaeoproterozoic plate tectonics. *Precamb. Res.* 304,
879 1-11.
- 880 Macgregor, A. M. 1951. "Some milestones in the Precambrian of Southern Rhodesia." *The*
881 *Transactions and Proceedings of the Geological Society of South Africa* 54: 39-50.
- 882 Martínez Catalán, J.R., Arenas, R., Abati, J., Sánchez Martínez, S., Díaz García, F., Fernández
883 Suárez, J., González Cuadra, P., Castiñeiras, P., Gómez Barreiro, J., Díez Montes, A., González
884 Clavijo, E., Rubio Pascual, F.J., Andonaegui, P., Jeffries, T.E., Alcock, J.E., Díez Fernández,
885 R., López Carmona, A., 2009. A rootless suture and the loss of the roots of a mountain chain:
886 the Variscan belt of NW Iberia. *C.R. Geosci.* 341, 114–126.
- 887 Mattauer, M., Tapponier, P., Proust, F. 1977. Sur les mécanismes de formation des chaînes
888 intracontinentales. L'exemple des chaînes atlasiques du Maroc., *Bull. Soc. Géol. Fr.* (7) 19, 521-
889 526.
- 890 Matte, P., 1986. Tectonics and plate tectonics model for the Variscan belt of Europe,
891 *Tectonophysics*, 126, 329-374.
- 892 Matte, P., 2001. The Variscan collage and orogeny (480-290 Ma) and the tectonic definition of
893 the Armorica microplate: a review. *Terra Nova* 13, 122–128.
- 894 Meert, J.G., 2002, Paleomagnetic evidence for a Paleo-Mesoproterozoic supercontinent
895 Columbia. *Gondwana Research*, 5, 207–215.
- 896 Meert, J.G., 2012. What's in a name? The Columbia (Palaeopangea/Nuna) Supercontinent.
897 *Gondwana Research*, 21, 987–993.
- 898 Meert, J.G., 2014, Strange attractors, spiritual interlopers and lonely wanderers: the search for
899 pre-Pangæan supercontinents. *Geoscience Frontiers*, 5, 155–166.
- 900 Meert, J.G., and Santosh, M., 2017. The Columbia supercontinent revisited. *Gondwana*
901 *Research*, 50, 67–83.
- 902 Michard, A., Soulaïmani, A., Hoepffner, C., Ouanaïmi, H., Baidder, L., Rjimati, E.C., Saddiqi,
903 O. 2020. The South-Western Branch of the Variscan Belt: Evidence from Morocco.
904 *Tectonophysics*, 492, 1–24.
- 905 Missenard Y., Zeyen H., Frizon de Lamotte D., Leturmy P., Petit C., Sébrier M., Saddiqi O.
906 2006. Crustal versus asthenospheric origin of the relief of the Atlas mountains of Morocco, J.
907 *Geophys. Res.* 111 (B03401) doi:10.1029/2005JB003708

- 908 Möller, A., Appel, P., Mezger, K. and Schenk, V. 1995. Evidence for a 2 Ga subduction zone:
909 eclogites in the Usagaran belt of Tanzania. *Geology* 23(12), 1067-1070.
- 910 Moyen, J.-F., Stevens, G. and Kisters, A. 2006. "Record of mid-Archaean subduction from
911 metamorphism in the Barberton terrain, South Africa." *Nature* 442(7102): 559-562.
- 912 Müller, S., Dziggel, A., Kolb, J., and Sindern, S., 2018, Mineral textural evolution and PT-path
913 of relict eclogite-facies rocks in the Paleoproterozoic Nagssugtoqidian Orogen, South-East
914 Greenland. *Lithos*, 296–299, 212–232.
- 915 Najman, Y., Jenks, D., Godin, L., Boudagher-Fadel, M., Millar, I., Garzanti, E., Horstwood,
916 M., Braccial, L., 2017. The Tethyan Himalayan detrital record shows that India–Asia terminal
917 collision occurred by 54 Ma in the Western Himalaya. *Earth and Planetary Science Letters*,
918 459, 301–310.
- 919 Nance, R., D., Gutiérrez-Alonso, G. Keppie, J., D., Linnemann, U., Murphy, J., B. Quesada,
920 C., Strachan, R., A. and Woodcock, N., A. 2010. Evolution of the Rheic Ocean. *Gondwana*
921 *Research*, 17, 194-222.
- 922 Nutman, A. Phillip., Kalsbeek, F. & Friend, C.R.L., 2008b. The Nagssugtoqidian orogen in
923 South-East Greenland: evidence for Paleoproterozoic collision and plate assembly. *American*
924 *Journal of Science*, 308, 529–572.
- 925 Nutman, A.P., Dawes, P.R., Kalsbeek, F., and Hamilton, M.A., 2008a. Palaeoproterozoic and
926 Archaean gneiss complexes in northern Greenland: Palaeoproterozoic terrane assembly in the
927 High Arctic. *Precambrian Research*, 161, 419–451.
- 928 Palin, R. M., Santosh, M., Cao, W., Li, S. S., Hernández-Uribe, D., & Parsons, A., 2020. Secular
929 metamorphic change and the onset of plate tectonics. *Earth-Science Reviews*, 103172.
- 930 Park, R. G. 2000. Mountain-building (orogenesis) in: *The Oxford Companion of the Earth*, p
931 707. Oxford University Press, 1174 pp.
- 932 Park, R.G., 1995. Paleoproterozoic Laurentia-Baltic relationships: a view from the Lewisian,
933 in Coward M.P., and Ries, A.C., eds., *Early Precambrian processes*. Geological Society,
934 London, Special Publication 95, 211–224.
- 935 Perchuk, A. L. and Morgunova, A. A. (2014). "Variable P-T paths and HP-UHP metamorphism
936 in a Precambrian terrane, Gridino, Russia: Petrological evidence and geodynamic
937 implications." *Gondwana Research* 25(2): 614-629.
- 938 Pesonen, L.J., Elming, S.-Å., Mertanen, S., Pisarevsky, S.A., D'Agrella-Filho, M.S., Meert,
939 J.G., Schmidt, P.W., Abrahamsen, N., and Bylund, G., 2003. Palaeomagnetic configuration of
940 continents during the Proterozoic. *Tectonophysics*, 375, 289–324.
- 941 Petrov, O., Shokalsky, S., Pospelov, I., Kashubin, S., Morozov, A., Sobolev, N., Petrov, E.,
942 Baluev, A., Sokolov, S., Grikurov, G., Vernikovskiy, V., St-Onge, M., Harrison, C., Ernst, R.,
943 Guarnieri, P., Labrousse, L., Lemmonier, N., Pubellier, M., Piepjohn, K., Smelror, M., Brekke,
944 H., Faleide, J., Stephens, M., Moore, T., Box, S., Grantz, A., and Orndorff, R., 2018. Tectonic
945 Map of the Arctic: CGMW-VSEGEI, doi:10.14683/2018TEMAR10M.
- 946 Pin, C. 1990. Variscan oceans: ages, origins and geodynamic implications inferred from
947 geochemical and radiometric data, *Tectonophysics*, 177, 215-227.

- 948 Piper, J.D.A., 1976, Paleomagnetic evidence for a Proterozoic supercontinent. *Philosophical*
949 *Transactions of the Royal Society of London*, A280, 469–490.
- 950 Pourteau, A., Candan, O. and Oberhänsli, R. 2010. High-Pressure metasediments in central
951 Turkey: constraints on the Neotethyan closure history. *Tectonics*, doi:10.1029/2009TC002650.
- 952 Pubellier, M., Meresse, F. 2013, Phanerozoic Growth of Asia; Geodynamic Processes and
953 Evolution. *Journal of Asian Earth Sciences*, 72, 118-128, doi: 10.1016/j.jseaes.2012.06.01.
- 954 Pubellier, M., Savva, D, Sapin, F., Aurelio, M., 2016. Structural Map of the South China Sea;
955 scale 1:3M, Commission for the Geological Map of the World,
956 doi:10.14682/2017STRUCTUSCS.
- 957 Puchkov, V. N., 2009. The evolution of the Uralian orogen. Geological Society, London,
958 *Special Publications*, 327(1), 161-195.
- 959 Robert, B., Domeier, M., and Jakob, J. 2020. Iapetan Oceans: An analog of Tethys? *Geology*.
- 960 Robert, C. and Bousquet, R. 2018. *Geowissenschaften: Die Dynamik des Systems Erde*.
961 Springer-Spektrum, 1016 pp
- 962 Roman A, Arndt N., 2019. Differentiated Archean oceanic crust: its thermal structure,
963 mechanical stability and a test of the sagduction hypothesis. *Geochim. Cosmochim. Acta*.
964 <https://doi.org/10.1016/j.gca.2019.07.009>
- 965 Schmid S. M., Bernouilli, D, Fügenschuh, B., Mattenco, L., Schefer, S., Schuster, R., Tischler,
966 M. and Ustaszewski, K., 2008. The Alpine-Carpathian-Dinaridic orogenic system; correlation
967 and evolution of tectonic units. *Swiss J. Geosci.* 101, 139-183. doi: 10.1007/s00015-008-1247-
968 3.
- 969 Schmid, S. M., Fügenschuh, B., Kounov, A. et al., 2019. Tectonic units of the Alpine collision
970 zone between Eastern Alps and western Turkey, *Gondwana Research*.
971 <https://doi.org/10.1016/j.gr.2019.07.005>
- 972 Scotese, C. R. 2016. PALEOMAP Paleo Atlas for GPLates and the Paleo Data Plotter Program,
973 PALEOMAP Project, <http://www.earthbyte.org/paleomap-paleoatlas-for-gplates/>
- 974 Scotese, C. R., 1991. Jurassic and Cretaceous plate tectonic reconstructions. *Palaeogeography,*
975 *Palaeoclimatology, Palaeoecology*, 87(1-4), 493-501.
- 976 Şengör, A. M. C., 1979. Mid-Mesozoic closure of Permo-Triassic Tethys and its implications.
977 *Nature* 279, 590-593.
- 978 Sengör, A. M. C., Natal'in, B. A., 1996. Paleotectonics of Asia: fragments of a synthesis. In:
979 Yin, A., Harrison, M. (Eds.), *The Tectonic Evolution of Asia*. Cambridge University Press,
980 Cambridge, pp. 486-640.
- 981 Sengör, A. M. C., Natal'in, B. A., Burtman, V. S., 1993. Evolution of the Altaid tectonic collage
982 and Palaeozoic crustal growth in Eurasia. *Nature* 364, 299-307.
- 983 Şengör, A. M. C., Yılmaz Y., 1981. Tethyan evolution of Turkey: A Plate Tectonics approach.
984 *Tectonophysics* 75, 181-241.
- 985 Sharkov, E., Lebedev, V., Chugaev, A., Zabarinskaya, L., Rodnikov, A., Sergeeva, N. and
986 Safonova, I. 2015. The Caucasian-Arabian segment of the Alpine-Himalayan collisional belt:
987 *Geology, volcanism and neotectonics. Geoscience Frontiers*, 503-522.
- 988 Shirey, S. B. and Richardson, S. H. 2011. Start of the Wilson cycle at 3 Ga shown by diamonds
989 from subcontinental mantle. *Science* 333(6041), 434-436.

- 990 Skublov, S. G. et al., 2011. New data on the age of eclogites from the Belomorian mobile belt
991 at Gridino settlement area. In *Doklady Earth Sci.* 439, 1163-1170.
- 992 Slabunov, A. I., Volodichev, O. I., Skublov, S. G. and Berezin, A. V. 2011. Main stages of the
993 formation of paleoproterozoic eclogitized gabbro-norite: Evidence from U-Pb (SHRIMP) dating
994 of zircons and study of their genesis. In *Doklady Earth Sci.* 437, 396 ().
- 995 Smithies, R., Champion, D. and Cassidy, K. 2003. "Formation of Earth's early Archaean
996 continental crust." *Precambrian Research* 127(1): 89-101.
- 997 Smoot C. 2012. *Tectonic Globaloney: Closing Arguments*. Author House. 158 pp.
- 998 Snoeyenbos, D. R., Williams, M. L., & Hanmer, S., 1995. Archean high-pressure
999 metamorphism in the western Canadian Shield. *European Journal of Mineralogy-Ohne*
1000 *Beihefte*, 7(6), 1251-1272.
- 1001 Stampfli, G. M., & Borel, G. D., 2002. A plate tectonic model for the Paleozoic and Mesozoic
1002 constrained by dynamic plate boundaries and restored synthetic oceanic isochrons. *Earth and*
1003 *Planetary Science Letters*, 196(1-2), 17-33.
- 1004 Stampfli, G. M., 2000. Tethyan oceans. *Geological Society of London Special Publications*
1005 173, 1-23.
- 1006 Stampfli, G. M., and Borel, G. D., 2004. The TRANSMED Transects in Space and Time:
1007 Constraints on the Paleotectonic Evolution of the Mediterranean Domain. In: Cavazza W. et al.
1008 *The TRANSMED Atlas*. Springer, p. 53-80.
- 1009 Stampfli, G. M., von Raumer, J. and Borel, G., D. 2002. Paleozoic evolution of pre-Variscan
1010 terranes: from Gondwana to the Variscan collision. *Geological Society of America, Special*
1011 *Paper* 364, 263-280.
- 1012 Stampfli, G., M. and Borel, G., D. 2002. A plate tectonic model for the Paleozoic and Mesozoic
1013 constrained by dynamic plate boundaries and restored synthetic oceanic isochrons. *Earth and*
1014 *Planetary Science Letters* 196, 17-33.
- 1015 Stille, H. 1920. Die Begriffe Orogenese und Epiorogenese: *Deutsch. Geol. Gesell. Zeitsch.* 71,
1016 164-240.
- 1017 Stille, H. 1940. *Einführung in den Bau Amerikas*: Berlin, Borntraeger, 717.
- 1018 St-Onge, M.R., Scott, D.J., Rayner, N., Sanborn-Barrie, M., Skipton, D.R., Saumur, B.M.,
1019 Wodicka, N., and Weller, O.M., 2020. Archean and Paleoproterozoic Cratonic Rocks of Baffin
1020 Island: In "Baffin Island and the Labrador-Baffin Seaway Geological Synthesis". (ed.) L. T.
1021 Dafoe & N. Bingham-Koslowski. *Geological Survey of Canada Bulletin*, 608, 01–29.
- 1022 St-Onge, M.R., Searle, M.P., and Wodicka, N., 2006. Trans-Hudson orogen of North America
1023 and Himalaya-Karakoram-Tibetan orogen of Asia: structural and thermal characteristics of the
1024 lower and upper plates. *Tectonics*, 25, 1–22.
- 1025 St-Onge, M.R., Van Gool, J.A.M., Garde, A.A., and Scott, D.J., 2009. Correlation of Archaean
1026 and Palaeoproterozoic units between northeastern Canada and western Greenland: constraining
1027 the pre-collisional upper plate accretionary history of the Trans-Hudson orogen. *Geological*
1028 *Society, London, Special Publication* 318, 193–235.

- 1029 St-Onge, M.R., Wodicka, N., and Ijewliw, O, 2007. Polymetamorphic evolution of the Trans-
1030 Hudson Orogen, Baffin Island, Canada: Integration of petrological, structural and
1031 geochronological data. *Journal of Petrology*, 48, 271–302.
- 1032 Strachan R.A., and Woodcock N.H., 2021. The Tectonic Pattern of Britain and Ireland. In:
1033 Alderton, David; Elias, Scott A. (eds.) *Encyclopedia of Geology*, 2nd edition. 4, 328-337.
1034 United Kingdom: Academic Press.
- 1035 Suess, E., 1893. Are Great Ocean Depth Permanent ? *Natural Science*, 2123, 180-187.
- 1036 Tang M, LeeC-TA, Rudnick RL, Condie KC., 2019. Rapid mantle convection drove massive
1037 crustal thickening in the late Archean. *Geochim. Cosmochim. Acta*.
1038 <https://doi.org/10.1016/j.gca.2019.03.039>
- 1039 Tardy, M., Blanchet, R., Zimmermann, M. 1989. The Texas and Caltam Lineaments from the
1040 American Cordillera to the Mexican Sierra Madres, nature, origin and structural evolution, p.
1041 219-226. In; Open-File Report 385, Geological study of the North American Cordillera, Bull.
1042 Centres Rech. Explor.-prod. Elf-Aquitaine, 13, 2., ISSN 0396-2687 – BCREDP
- 1043 Taylor, B., Goodliffe, A. M. and Martinez, F., 1999. How continents break up: insights from
1044 Papua New Guinea. *Journal of Geophysical Research: Solid Earth*, 104(B4), pp.7497-7512.
- 1045 Taylor, S. R., McLennan, S. M., 1985. *The Continental Crust: Its Composition and Evolution*.
1046 Blackwell Scientific Publication, Carlton, 312 pp. OSTI ID: 6582885.
- 1047 Thébaud, N., & Rey, P. F., 2013. Archean gravity-driven tectonics on hot and flooded
1048 continents: controls on long-lived mineralised hydrothermal systems away from continental
1049 margins. *Precambrian Research*, 229, 93-104.
- 1050 Thompson, D.A., Bastow, I.D., Helffrich, G., Kendall, J-M., Wookey, J., Snyder, D.B., and
1051 Eaton, D.W., 2010. Precambrian crustal evolution: seismic constraints from the Canadian
1052 Shield. *Earth and Planetary Science Letters*, 297, 655–666.
- 1053 Thurmann, M. J. 1854. Résumé des lois orographiques générales du système des monts Jura :
1054 *Soc. Geol. France Bull.*, 2, 11, 41-57.
- 1055 Tugend, J., Manatschal G., Kuszniir, N. J. Masini E., Mohn, G., et al. 2014. Formation and
1056 deformation of hyperextended rift systems: Insights from rift domain mapping in the Bay of
1057 Biscay-Pyrenees. *Tectonics*, American Geophysical Union (AGU), 33, pp.1239-1276.
1058 (10.1002/2014TC003529)
- 1059 Upham, W. 1894. Wave-like progress of an epeirogenic uplift: *Jour. Geology*, 2, 380-395.
- 1060 Van Gool, J.A.M., Connelly, J.N., Marker, M., and Mengel, F.C., 2002. The Nagssugtoqidian
1061 Orogen of West Greenland: Tectonic evolution and regional correlations from a West Greenland
1062 perspective. *Canadian Journal of Earth Sciences*, 39, 665–686.
- 1063 Van Kranendonk, M. J., Collins, W. J., Hickman, A., Pawley, M. J., 2004. Critical tests of
1064 vertical vs. horizontal tectonic models for the Archaean East Pilbara granite-greenstone terrane,
1065 Pilbara craton, Western Australia. *Precambrian Res.* 131 (3), 173–211.
- 1066 Volodichev, O. I., Slabunov, A. I., Bibikova, E. V., Konilov, A. N. and Kuzenko, T. I. 2004.
1067 Archean eclogites in the Belomorian mobile belt, Baltic Shield. *Petrology* 12(6), 540-560.

- 1068 Wan, B., Windley, B. F., Xiao, W., Feng, J., Zhang, J., 2015. Paleoproterozoic high-pressure
1069 metamorphism in the northern North China Craton and implications for the Nuna
1070 supercontinent. *Nat. Commun.* 6, 8344.
- 1071 Wan, B., Yang, X., Tian, X., Yuan, H., Kirscher, U., and Mitchell, R.N., 2020. Seismological
1072 evidence for the earliest global subduction network at 2 Ga ago. *Science Advances*, 6.
1073 eabc5491.
- 1074 Wang, Y., Fan, W., Zhang, G., & Zhang, Y. 2013. Phanerozoic tectonics of the South China
1075 Block: key observations and controversies. *Gondwana Research*, 23(4), 1273-1305.
1076
- 1077 Weissel, J. K., & Watts, A. B. 1979. Tectonic evolution of the Coral Sea basin. *Journal of*
1078 *Geophysical Research: Solid Earth*, 84(B9), 4572-4582.
- 1079 Weller, O.M., and St-Onge, M.R., 2017. Record of modern-style plate tectonics in the
1080 Palaeoproterozoic Trans-Hudson orogeny. *Nature Geoscience*, 10, 305–313.
- 1081 Weller, O.M., Jackson, S., Miller, W.G.R., St-Onge, M.R., and Rayner, N., 2020. Quantitative
1082 elemental mapping of granulite- facies monazite: Textural insights and implications for
1083 petrochronology. *Journal of Metamorphic Geology*, 38, 853–880.
- 1084 Wilson, R. W., Houseman, G. A., Buitter, S. J. H., McCaffrey, K. J. W. and Doré, A. G. 2019.
1085 Fifty years of the Wilson Cycle Concept in Plate Tectonics: an Overview. Geological Society,
1086 London, Special Publications. DOI: <https://doi.org/10.1144/SP470-2019-58>
- 1087 Xiao, W. J., Han, C. M., Yuan, C., Sun, M., Lin, S. F., Chen, H. L., Li, Z. L., Li, J. L., and Sun,
1088 S., 2008. Middle Cambrian to Permian subduction-related accretionary orogenesis of North
1089 Xinjiang, NW China: implications for the tectonic evolution of Central Asia. *Journal of Asian*
1090 *Earth Sciences*, 32, 102-117.
- 1091 Xin Y., Li J., Ratschbacher L., Zhao G., Zhang Y., Dong S., Xia X-P., Yu Y. 2020. Early
1092 Devonian (415 -400 Ma) A-type granitoids and diabases in the Wuyishan, eastern Cathaysia:
1093 A signal of crustal extension coeval with the separation of South China from Gondwana. *Geol.*
1094 *Soc. Am. Bull.*
- 1095 Xu, C., Kynický, J., Song, W., Tao, R., Lü, Z., Li, Y. and Fei, Y. 2018. Cold deep subduction
1096 recorded by remnants of a Paleoproterozoic carbonated slab. *Nature communications*, 9(1),
1097 2790.
- 1098 Yao W., Li ZX., Li WX. 2014. Was there a Cambrian ocean in South China? – Insight from
1099 detrital provenance analyses. *Geol. Mag.* 1-8 Cambridge University Press
1100 doi:10.1017/S0016756814000338.
- 1101 Yu, H.L., Zhang, L.F., Wei, C.J., Li, X.L., and Guo, J.H., 2017. Age and P–T conditions of the
1102 Gridino-type eclogite in the Belomorian Province, Russia. *Journal of Metamorphic Geology*,
1103 35, 855–869.
- 1104 Zhao, G. and Cawood, P., 1999. Tectonothermal evolution of the Mayuan assemblage in the
1105 Cathaysia Block: implications for Neoproterozoic collision-related assembly of the South
1106 China Craton. *Am. J. Sci.*, 299, 309–339.
- 1107 Zhao, G., Cawood, P.A., Wilde, S.A., and Sun, M., 2002. Review of global 2.1–1.8 Ga orogens:
1108 implications for a pre-Rodinia supercontinent. *Earth-Science Reviews*, 59, 125–162.

- 1109 Zhao, G., Li, S., Sun, M., and Wilde, S.A., 2011. Assembly, accretion, and break-up of the
1110 Palaeo-Mesoproterozoic Columbia supercontinent: record in the North China Craton revisited.
1111 *International Geology Review*, 53, 1331–1356.
- 1112 Zhao, G., Sun, M., Wilde, S.A., and Li, S., 2004. A Paleo-Mesoproterozoic supercontinent:
1113 assembly, growth and breakup. *Earth-Science Reviews*, 67, 91–123.